REVIEW

Check for updates

Smart stimuli-responsive polysaccharide nanohydrogels for drug delivery: a review

Fouad Damiri, [ID] *[ab] Ahmed Fatimi,*[a] Ana Cláudia Paiva Santos, [ID] [cd] Rajender S. Varma[e] and Mohammed Berrada*[b]

Polysaccharides have found extensive utilization as biomaterials in drug delivery systems owing to their remarkable biocompatibility, simple functionalization, and inherent biological properties. Within the array of polysaccharide-based biomaterials, there is a growing fascination for self-assembled polysaccharide nanogels (NG) due to their ease of preparation and enhanced appeal across diverse biomedical appliances. Nanogel (or nanohydrogel), networks of nanoscale dimensions, are created by physically or chemically linking polymers together and have garnered immense interest as potential carriers for delivering drugs due to their favorable attributes. These include biocompatibility, high stability, the ability to adjust particle size, the capacity to load drugs, and their inherent potential to modify their surface to actively target specific cells or tissues *via* the attachment of ligands that can recognize corresponding receptors. Nanogels can be engineered to respond to specific stimuli, such as pH, temperature, light, or redox conditions, allowing controlled release of the encapsulated drugs. This intelligent targeting capability helps prevent drug accumulation in unintended tissues and reduces the potential side effects. Herein, an overview of nanogels is offered, comprising their methods of preparation and the design of stimulus-responsive nanogels that enable controlled release of drugs in response to specific stimuli.

1. Introduction

Each year, a significant portion of the world's population undergoes treatments for cancer, diabetes mellitus,[1] neurodegenerative diseases, and cardiovascular conditions. Unfortunately, these treatments often come with side effects that negatively impact the overall well-being of the individuals. Consequently, it is crucial to explore alternative approaches for both diagnosing and treating diseases in order to reduce these adverse effects. Nanotechnologies, encompassing focused administration of drugs, heat treatment, light-based assays, light-induced therapy, and tissue engineering, have been considered to be encouraging methodologies to tackle the drawbacks of existing

techniques.[2,3] These advancements hold promise in providing potential solutions to surmount these obstacles.

Nanohydrogels (NHs), or nanogels, are polymer networks with a size smaller than a micron and comprise hydrogel particles with a nanometer-scale space, exhibiting characteristics of both hydrogels and nanoparticles. In the realm of nanoparticles, which consists of inorganic, lipid, and polymer nanoparticles, nanogels fall into the latter category. To create nanohydrogels, one can either use polymeric precursors or carry out polymerization of monomers under heterogeneous conditions, with cross-linking being a crucial step. Nanohydrogels possess hydrophilic functionalities such as $-SO_3H$, $-OH$, $-CONH_2-$, and $-CONH-$, which enable them to absorb considerable quantities of biological fluids or water at the same time as preserving their organizational integrity. However, due to the existence of cross-links, nanogels expand instead of dissolving upon contact with a solvent. This remarkable characteristic makes nanogels highly promising for a wide range of applications. Numerous research studies have showcased the appropriateness of nanogels as carriers for drug delivery.[4] This is attributed to their exceptional ability to accommodate a substantial quantity of drugs, maintain a high level of stability, exhibit biocompatibility, and respond to numerous environmental elements, namely ionic strength, pH, and temperature, in a superior manner relative to conventional pharmaceutical nanocarriers.

[a] *Chemical Science and Engineering Research Team (ERSIC), Department of Chemistry, Polydisciplinary Faculty of Beni Mellal (FPBM), University Sultan Moulay Slimane (USMS), Beni Mellal 23000, Morocco. E-mail: fouad.damiri@outlook.fr*

[b] *Laboratory of Biomolecules and Organic Synthesis (BIOSYNTHO), Department of Chemistry, Faculty of Sciences Ben M'Sick, University Hassan II of Casablanca, Casablanca 20000, Morocco. E-mail: a.fatimi@usms.ma*

[c] *Department of Pharmaceutical Technology, Faculty of Pharmacy of the University of Coimbra, University of Coimbra, Coimbra, Portugal*

[d] *REQUIMTE/LAQV, Group of Pharmaceutical Technology, Faculty of Pharmacy of the University of Coimbra, University of Coimbra, Coimbra, Portugal*

[e] *Centre of Excellence for Research in Sustainable Chemistry, Department of Chemistry, Federal University of São Carlos, 13565-905 São Carlos – SP, Brazil. E-mail: berrada_moh@hotmail.com*

10538 | *J. Mater. Chem. B*, 2023, **11**, 10538–10565

This journal is © The Royal Society of Chemistry 2023

Extensive research endeavors have focused on investigating stimulus-responsive nanogels in the past decade, resulting in their noteworthy impact on the advancement of drug transport systems (Fig. 1). Nanogels have emerged as targeted nanocarriers that enable precise and controlled release of drugs, thereby improving drug stability in the field of nanomedicine. These nanohydrogels, composed of hydrophilic polymeric systems with a size range below one micron, serve as efficient vehicles for drug delivery. Most nanogels reported previously, however, are not biodegradable, and their synthesis often entails the use of surfactants.[5] They possess viscoelastic characteristics and are formed through either non-covalent interactions or covalent bonding between polymer chains. When exposed to an aqueous medium, nanohydrogels tend to absorb water. While their internal structure resembles hydrogels and polyelectrolyte microgels, nanogels differ primarily in size and the kind of reaction deployed in their synthesis. Nanohydrogels possess distinctive qualities that make them ideal for various applications. They exhibit biocompatibility, ensuring compatibility with living systems, and offer exceptional stability.[6] Moreover, their

Fouad Damiri

Dr Fouad Damiri earned his PhD in Organic and Polymer Chemistry from Hassan II University of Casablanca, Morocco in 2021 under the supervision of Prof. Mohammed Berrada. His research focuses on the development of smart nano biomaterials based on polysaccharides for the drug delivery systems. He actively contributes as a member of editorial and a reviewer for numerous international journals. Dr Fouad Damiri has authored over 27 papers and 11 book chapters, which have collectively garnered 491 citations.

Ahmed Fatimi

Dr Ahmed Fatimi is an associate professor at Sultan Moulay Slimane University (Morocco). He has a Master's degree (chemical engineering) from Polytech'Nantes School (France) and a Master's degree (biopolymers engineering) from the University of Nantes (France). In 2008, he obtained a PhD degree in biomaterials from the University of Nantes on the rheological behavior of biomaterials for osteoarticular and dental tissue engineering. From 2009 to 2012, he worked as a post-doctoral research fellow at the Canada Research Chair in Biomaterials and Endovascular Implants. Dr Fatimi's research is focused on the development and formulation of hydrogels for tissue engineering and biomedical use and their physico-chemical and rheological properties. Dr Fatimi is also interested in intellectual property aspects, particularly patents and their analysis. He is the inventor of 8 patents, has published 44 articles and 7 book chapters, and has presented around 80 conference communications.

Rajender S. Varma

Prof. Rajender Varma (h-index 130, Highly Cited Res. 2016, 18, 19, 20, 21, 22) born in India (PhD, Delhi University 1976) has been a senior scientist at U.S. EPA since 1999. He has over 50 years of multidisciplinary research experience ranging from eco-friendly synthetic methods using microwaves, ultrasound, etc. to greener assembly of nanomaterials and sustainable appliances of magnetically retrievable nanocatalysts in benign media. He is a member of the editorial advisory board of several international journals, has published over 955 papers, and awarded 17 U.S. Patents, 9 books, 29 book chapters, and 3 encyclopedia contributions with 69600 citations.

Mohammed Berrada

Dr Mohammed Berrada stands as an eminent trailblazer within the realm of polymer science, celebrated for his extensive involvement in a myriad of university-industry technology transfer initiatives. At present, he holds the prestigious position of Head of the Innovation and Technology Platform at Hassan II University in Casablanca, Morocco, simultaneously fulfilling the role of a distinguished professor specializing in Organic Chemistry and Polymer Science. Dr Berrada's unwavering devotion to pushing the boundaries of polymer science is underscored by his remarkable track record in both academic and industrial spheres. His exceptional contributions reverberate throughout the field, consistently reshaping and redefining the landscape of polymer research and innovation.

This journal is © The Royal Society of Chemistry 2023

*J. Mater. Chem. B*, 2023, **11**, 10538–10565 | **10539**

Fig. 1 A visual representation of nanogels responding to specific stimuli and their application in delivering therapeutic substances (created with https://BioRender.com).

particle size can be easily adjusted as needed. Additionally, nanohydrogels are capable of responding to external factors like temperature, pH, light, and ionic strength, thus enhancing their versatility. These exceptional attributes make nanogels well-suited for diverse uses, such as tissue engineering, biomedical implants, gene therapy, and the delivery of medications.[7]

Polysaccharides are sourced from several natural sources, like animals, plants, microbes, and algae.[4,8,9] Consequently, nanogels (NG) constructed from biocompatible and biodegradable polymers show immense potential for utilization in drug delivery systems (DDS).[4] Moreover, polysaccharide-derived NGs offer excellent biocompatibility, functionality, adjustable size, ample surface area for bioconjugation, and an inner network that allows for precise regulation of the integration and release of bioactive compounds.[10] Biopolymeric nanocarriers are created using natural polymers, like cellulose,[11] chitosan,[12] sodium alginate,[13] and hyaluronic acid,[14] as well as synthetic polymers, namely polylactic acid (PLA),[15] polyacrylamide (PAA),[16] poly(lactide-co-glycolide) (PLGA),[17] and polyglycolic acid (PGA),[18] dendrimers,[19] among others.

Intelligent stimuli-responsive polysaccharide nanohydrogels for drug delivery have garnered significant consideration

Dr Ana Cláudia Paiva-Santos obtained her PhD degree in Pharmaceutical Nanotechnology in 2018. She started her pedagogical intervention as a Teaching Assistant during the PhD, and then became an Invited Assistant Professor. Since 2020 she has been an Assistant Professor at the Faculty of Pharmacy of the University of Coimbra (FFUC), where she teaches Pharmaceutical Technology and Nanotechnology. She has published >120 papers and 12 book chapters in nanotechnology and nanomedicine, and submitted one patent application, as a result of work performed with several national and international collaborations (h-index 23). She was among the World's Top 2% of Scientists in 2022 as determined by Stanford University.

recently. These nanohydrogels, comprising biocompatible and biodegradable polysaccharides, offer promising potential for enhancing drug delivery systems. Herein, a comprehensive overview is offered for the synthesis, characterization, and applications of these intelligent nanohydrogels, besides an exploration of their response to different stimuli like temperature, pH, enzymes, and external triggers.[20] Furthermore, the benefits, obstructions, and potential future advancements of utilizing these nanohydrogels in the field of drug delivery are discussed. The advancements in this field are highlighted by exploring the progress made in intelligent stimuli-responsive nanohydrogels derived from polysaccharides, with the ultimate goal of facilitating the growth of these nanohydrogels for effective drug delivery applications.[21,22]

Nevertheless, the evaluation also highlighted their usage in the transportation of drugs and genes, photodynamic treatment, biological imaging, and biological sensing, with the primary emphasis being on the various types of responsive nanogels, especially those triggered by redox reactions, temperature changes, pH, and light. Simultaneously, it addressed the challenges that need to be circumvented to achieve successful cancer therapy (Fig. 1).

2. Aspects related to the synthesis of stimuli-responsive nanohydrogels

There are two main types of nanoparticle gels (NGs) that respond to various stimuli that can originate from within the body, such as changes in pH, bioreduction, or recognition of specific biomolecules, or can be triggered by external factors like temperature, light, ultrasound, or a magnetic field. The production of "smart" NGs typically involves polymerizing specific functional monomers or utilizing the polymerization of natural polymers that have been modified with functional groups (Table 1). This process is often combined with other synthesis methods and followed by cross-linking.[4] NGs can undergo cross-linking via physical or chemical approaches. As mentioned earlier, the physical cross-linking involves non-covalent interactions, and the stability of the resulting physically cross-linked NGs depends on factors such as the composition of the monomer or polymer and the density of cross-linking attained in the course of production. In contrast, chemical cross-linking utilizes "ideal crosslinkable" molecules that form connections with the polymer chains. This method provides accurate manipulation of NG characteristics and represents a promising approach for generating stable NGs without the requirement of supplementary substances like surfactants. Covalent cross-linking has specific advantages in regulating NG strength, structure, and swelling behavior, which are vital for controlled loading and the programmed release of therapeutic and theranostic substances. Over the last ten years, researchers have utilized a range of natural and synthetic polymers, along with cross-linking molecules or macromolecules, to create these dynamic nanogels (NGs). Fig. 2 showcases illustrations of the polymers and cross-linking molecules and macromolecules employed in the manufacturing process.[23]

10540 | *J. Mater. Chem. B*, 2023, **11**, 10538–10565

This journal is © The Royal Society of Chemistry 2023

Table 1 Polysaccharide-based nanogels for drug delivery systems

Polymer	Nanogel system	Therapeutics	Ref.
Chitosan	CTS-g-PHEMA-maleic acid	Doxorubicin (DOX)	24
	Chitosan/poly(N-isopropylacrylamide)	Gold nanoparticles (AuNPs)	25
	Trimethyl chitosan (TMC)/poly(2-hydroxyethyl methacrylate) (PHEMA)	Melatonin	12
Cellulose	Methacrylated monocarboxylic sugarcane bagasse cellulose (MAMC-SBC)/N-isopropylacrylamide (NIPAM)	Doxorubicin (DOX)	11
	Carboxymethyl nanocellulose (CMNC)/lysozyme	Acyclovir, carbamazepine, and furosemide	26
	(CDs/DCMC-Gel)-FA	Curcumin (CUR)/doxorubicin (DOX)	27
Starch	Carboxymethyl starch-lysozyme	Epigallocatechin gallate (EGCG)	28
	Starch nanocrystals/gum Arabic	Hydroxyurea	29
	Fe$_3$O$_4$-g-(PNIPAAm-co-PMA)@starch	Doxorubicin (DOX)	30
Alginate	Alginate/chitosan (ACC)	Mupirocin	31
	Sodium alginate-chitosan (AO/CHPCS)	Berberine (BBR)	32
	Alginate	Doxorubicin (DOX)	33
Dextran	Dextran (Dex-CHO)/cystamine dihydrochloride (Cys)	Doxorubicin (DOX)	34
	SPI-SA-DX	Curcumin	35
	(Fe$_3$O$_4$@Dex)	—	36
Pectin	Lysozyme-pectin	Methotrexate (MTX)	37
	ALG-g-PHPMA@Et	Etoposide (Et)	38
	Ovalbumin-pullulan	Curcumin (Cur)	39
Hyaluronic acid	Maleoyl-chitosan/poly(aspartic acid)	Amoxicillin (Amox)	40
	(^{Ce6}HANG/DOX)	Doxorubicin (DOX)	41
	(Lf-DOX/PBNG)	Doxorubicin (DOX)	42
Carragenan	(CG or κ-carrageenan)	Rivastigmine tartrate (RIV)	43
	KCAR-NGs	Amoxicillin and iodixanol	44
	PN-NG@ION PAA-g-κC HG	Levodopa (L-DOPA)	45
Heparin	HEP	Doxorubicin (DOX)	46
	Heparin–Pluronic (Hep–Pr)	Paclitaxel and DNase	47
	HP403	Cisplatin/curcumin	48
Gellan gum	Gellan–cholesterol	Prednisolone (Pred)	49
	Gellan–prednisolone		
	Chitosan–gellan gum	Curcumin (Cur)	50
	Gellan gum (GG)/chitosan (CS)	Polymyxin B (PMB)	51
Xanthan gum	Cassava starch (CS)/xanthan gum (XG)	—	52
	Polyethylene glycol/xanthan gum-co-poly(acrylic acid)	Venlafaxine	53
	Xanthan gum (XG)/poly(AA)	Amoxicillin	54

3. Polysaccharide-based nanogels for drug delivery

Polysaccharides are types of carbohydrates characterized by their extensive polymeric oligosaccharide configurations. These structures are formed through glycosidic linkages, as illustrated in (Fig. 3), which connect several repeating units of monosaccharides. Polysaccharides are naturally occurring compounds that are found in a range of sources, such as plants, as exemplified by pectin, cellulose, and starch.[55] Animals also afford polysaccharides such as chitosan, chitin, and glycosaminoglycan.[56] The presence of microorganisms is pivotal in the production of diverse polysaccharides, which include notable examples like dextran, pullulan, xanthan gum, and gellan gum. Additionally, algae serve as a valuable source of polysaccharides like agar, alginate, and carrageenan (Fig. 3).
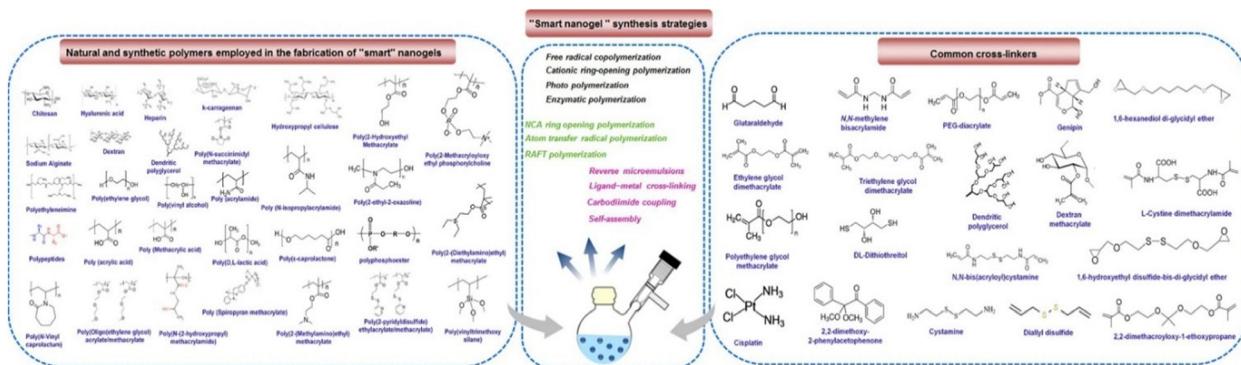

Fig. 2 Illustration of various synthetic approaches, natural as well as synthetic polymers and crosslinkers employed in the fabrication of stimuli-responsive polymer nanogels. Reproduced from ref. 23 with permission from Elsevier, copyright 2020.

This journal is © The Royal Society of Chemistry 2023

J. Mater. Chem. B, 2023, 11, 10538–10565 | 10541
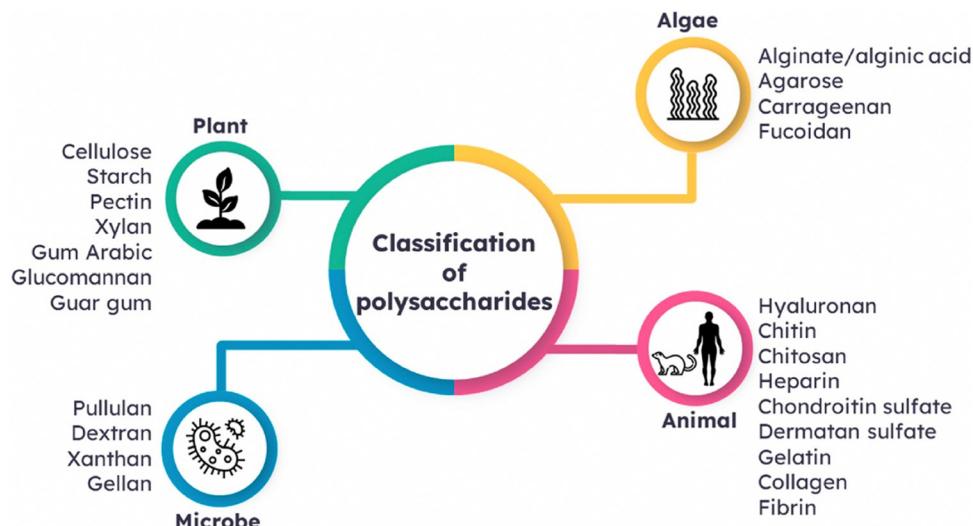
Fig. 3 Classification of polysaccharides based on their sources of origin. Reproduced from ref. 4 with permission from Elsevier, copyright 2023.

Natural polymers are favored over synthetic counterparts due to their readily available nature, susceptibility to chemical alterations, renewability, cost-effectiveness, non-toxicity, stability, hydrophilicity, biocompatibility, and biodegradability (Fig. 4). In contrast, synthetic polymers are relatively expensive and pose environmental and toxicity concerns, along with lengthy and involved synthetic processes.

3.1. Chitosan-derived nanogels

Chitosan, a cationic polyaminosaccharide, is obtained through the deacetylation process of chitin, which originates from various sources like crustaceans (such as crabs and shrimp), amphineuras (like chiton), archiannelida, fungi, and plants. This naturally derived substance can be dissolved and utilized in numerous appliances, including wound dressings, tissue engineering, drug delivery systems, biosensors, and medical implants.[57] Chitosan offers several advantages due to its natural origin, good

biocompatibility and biodegradability, bioadhesive properties, non-toxicity, non-immunogenicity, antibacterial and antifungal activities, responsiveness to stimuli, and affordability.[4,58,59]

Yao and colleagues[60] introduced an innovative nanogel/gel that exploited chitosan (CS) as a foundation for the oral delivery of myricetin (Myr); CS/β-glycerol phosphate (β-GP) nanogels loaded with Myr of particle sizes ranging from 100 to 300 nm.

3.2. Cellulose-based nanogels

Cellulose is a straight-chain polysaccharide composed of beta D-glucopyranose components arranged in a $^4C_1$ chair configuration and is formed by linking these units together through beta acetal linkages, termed beta-1,4-glycosidic bonds.[61] The linear structure of cellulose is a consequence of these linkages. Additionally, cellulose possesses three available hydroxyl groups, which enable the formation of hydrogen bonds within and between the cellulose chains.[62,63] Besides, cellulose, the
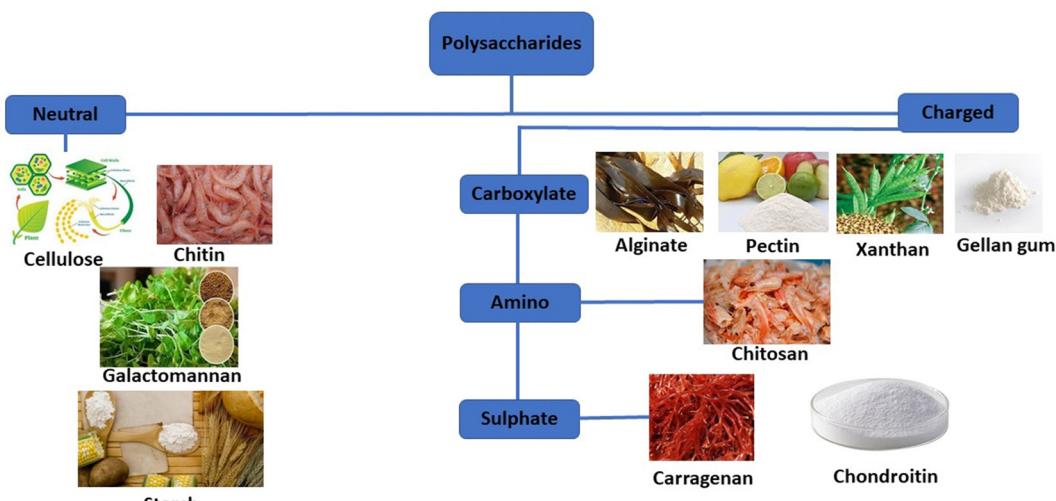

Fig. 4 The categorization of common polysaccharides that are widely deployed in the drug delivery field.

most prevalent biomass material found in nature, possesses remarkable biocompatibility and biodegradability. As a result, cellulose and its derivatives are highly regarded as promising options for fabricating nanogels utilized for drug delivery purposes.[11]

In their study, Pan et al.[11] created multi-responsive nanogels by utilizing a modified form of cellulose obtained from sugarcane bagasse (SBC). They deployed cystamine bisacrylamide (CBA) as a crosslinking agent and performed an in situ aqueous copolymerization (free radical) of methacrylated monocarboxylic sugarcane bagasse cellulose (MAMC-SBC) and N-isopropylacrylamide (NIPAM). This synthesis process resulted in the formation of nanogels that exhibit responsiveness to changes in redox conditions, pH levels, and temperature.

3.3. Starch-based nanogels

Due to their affordability, renewability, and biocompatibility, starch and its derivatives have played significant roles in various biomedical applications. Starch is a plentiful polysaccharide and is found in various plant sources such as seeds, beans, and tubers.[64] It is made up of two primary components, amylose and amylopectin. These constituents are comprised of glucose molecules interconnected by α-D-(1–6) glycosidic and/or α-D-(1–4) bonds. While amylose primarily possesses a linear structure with minimal branching, amylopectin makes up the majority of starch, accounting for over 75% of its composition.[65] Amylopectin consists not only of a chain of α-D-(1–4) glucose units but also of numerous branches that are linked by α-D-(1–6) glucose bonds.[66]

Sousa et al.[67] conducted a co-encapsulation synthesis to merge oncocalyxone A (onco A) and magnetite nanoparticles (Fe_3O_4@citrate) with modified surfaces, forming a unified nanostructure. The nanocapsules obtained displayed a core–shell structure and possessed an average diameter of 143 nm.

3.4. Alginate-derived nanogels

Alginate (ALG) is a linear polysaccharide characterized by non-uniform segments of β-D-mannuronic acid (M) and α-L-guluronic residues (G) linked together through 1–4 bonds.[68] Alginate is soluble in water and possesses a block-like structure, where it can exhibit either a homogeneous (poly-G, poly-M) or a heterogeneous pattern (MG).[69] The arrangement of monomers and their linkages in the polymer leads to diverse geometries in the M-block regions, G-block regions, and alternating regions.[70] The strength or brittleness of ALG gels can be impacted by augmenting the number of G blocks within alginate and increasing the polymer's molecular weight. Although alginic acid is insoluble in water or organic solvents, stable solutions are formed by utilizing monovalent alginate salts. However, if the pH falls below the pK_a range of 3.38–3.65, the alginate biopolymer precipitates. Moreover, factors like ionic strength and the presence of gelling ions can affect the solubility of alginate salts.

In this context, Suhail et al.[71] have created a network of nanogels using polymers to achieve a continuous release of caffeine. To attain this, they employed a free-radical polymerization method to fabricate alginate-based nanogels. To crosslink the alginate polymer, the monomer 2-acrylamido-2-methylpropanesulfonic acid was employed, along with the crosslinker N',N'-methylene bisacrylamide. Several analyses were performed on the synthesized nanogels, encompassing assessments of the sol–gel fraction, polymer volume fraction, swelling behavior, drug loading capacity, and drug discharge characteristics.

3.5. Dextran-based nanogels

Dextran, derived from microorganisms, is a polysaccharide composed of glucose units connected by α-1,6-glycosidic bonds. In addition, it comprises a minor portion of branches established via α-1,4, α-1,3, and α-1,2 linkages.[72,73] This adaptable substance can be readily altered to amplify its reactivity and functionality. In the food sector, dextran has found extensive use due to its stabilizing, emulsifying, viscosity-enhancing, and texturizing characteristics. Apart from its industrial applications, dextran exhibits considerable potential in the realm of biomedicine.[34] Dextran is widely utilized in various fields, including drug dispensation and tissue engineering. Specifically, dextran variants with molecular weights of 40, 60, and 70 kDa are commonly employed in biomedical applications owing to their high quality and suitability for clinical use.

In their study, Yu et al.[34] focused on the generation of dextran-based nanogels termed Dex-SS via a straightforward method that involved the formation of Schiff base bonds containing disulfide between polyaldehyde dextran and cystamine. This process occurred within a water-in-oil inverse microemulsion. The researchers analyzed the morphology of the treated nanogels using SEM imaging and investigated the degradation behavior of these nanogels under both acidic and reductive (GSH) conditions. To achieve controlled drug release, they covalently linked doxorubicin (DOX) to the dextran nanogels through Schiff base connections. As a result, the drug release profiles exhibited sensitivity to both pH and GSH, enabling a dual-responsive drug release mechanism.

3.6. Pectin-based nanogels

Pectin, which is a crucial element found in plant cell walls, is classified as a heteropolysaccharide. It is characterized by the presence of α-(1,4) galacturonic acid units, and this anionic polysaccharide exhibits a substantial molecular weight ranging from 60 000 to 130 000 g mol^{-1}.[74] Additionally, the pectin backbone also includes neutral sugars such as arabinose, rhamnose, galactose, and smaller quantities of additional sugars.[75,76] Pectin is known for its non-toxicity, biocompatibility, and role as a vital component in various biological processes.

In 2016, Zhou et al.[77] created protein/polysaccharide complexes that have captured significant attention due to their potential uses in the food industry, biomedicine, and pharmaceutics. In their research, they focused on developing new nanogels, measuring less than 60 nm, by utilizing a straightforward process involving the complexation of low-density lipoprotein (LDL) from egg yolk with pectin, induced by changes in pH and temperature. The team conducted a detailed examination of the nanostructure of egg yolk LDL under

This journal is © The Royal Society of Chemistry 2023

J. Mater. Chem. B, 2023, 11, 10538–10565 | 10543

varying pH conditions and thoroughly investigated its interaction with pectin.

3.7. Hyaluronic acid-derived nanogels

Hyaluronic acid (HA) is a glycosaminoglycan naturally present in the human body. It lacks sulfation and is primarily located in skin, connective tissues, and synovial joint fluids. HA is composed of repeating units of the disaccharide β-1,4-D-glucuronic acid – β-1,3 N-acetyl-D-glucosamine.[78] HA possesses various physicochemical characteristics, like its viscoelastic properties and remarkable abilities in water retention, making it highly suitable for medical applications due to its biocompatibility and bio-functionality.

Luan et al.[79] have developed nanogels capable of undergoing degradation in the presence of acidic environments and were synthesized in an aqueous medium using a surfactant-free polymerization technique, employing 2,2-dimethacroyloxy-1-ethoxypropane (DMAEP) as a cross-linker that is sensitive to pH changes. Through the adjustment of cross-linking degrees, nanogels with diverse properties were produced. The researchers successfully loaded the anti-cancer drug doxorubicin (DOX) into the nanogels, achieving drug-loading contents (DLC) ranging from 7.67% to 12.15%. Importantly, when subjected to acidic conditions, the nanogels demonstrated an accelerated release of DOX.

3.8. Carragenan-based nanogels

Carrageenan (CG) is a naturally occurring linear sulfated polysaccharide with a moderate to high molecular weight, typically ranging from 100 to 1000 kDa. It consists of a repetitive pattern of galactose and 3,6-anhydrogalactose, connected by alternating α-(1,3) and β-(1,4)-glycosidic bonds. CG can be classified into six main forms (κ, ï, η, μ, λ, and θ) based on its structural attributes. These forms differ in terms of solubility, the presence and position of sulfate groups (typically ranging from 22% to 35%), as well as the extraction method and source. In the pharmaceutical field, three specific forms of CG, namely κ, λ, and ï, have particular importance as they have been extensively studied and recognized for their diverse applications. These forms exhibit unique properties and functionalities that make them suitable for pharmaceutical purposes. Therefore, within the pharmaceutical industry, κ, λ, and ï forms of CG are highly regarded and extensively utilized.

Rahmani et al.[43] developed pH-responsive nanogels that incorporate rivastigmine as a representative drug model. The nanogels were created by the graft polymerizing method, deploying acrylamide and sodium acrylate monomers onto chitosan (CS) and kappa-carrageenan (CG or κ-carrageenan) structures. The synthesis procedure involved the utilization of N,N′-methylenebisacrylamide (MBA) as a cross-linker, along with ammonium persulfate and nitrogen-doped carbon dots (N-CDs) as initiators. Various techniques such as FTIR, FE-SEM, EDX, XRD, and TGA were employed to characterize the nanogels. The swelling performance of the nanogels was affected by factors like monomer content, MBA content, the quantity of CS or CG, and the pH conditions during synthesis. Notably, the nanogels demonstrated notable responsiveness to pH in drug

release experiments, with a drug release of less than 61% observed under simulated gastric conditions (pH 1.2) and ~95% under imitation intestinal conditions (pH 7.4).

3.9. Heparin-based nanogels

Heparin is composed of sulfated disaccharides that repeat and form a polysaccharide, wherein the constituent disaccharides are made up of pyranosyluronic acid and glucosamine residues. Heparin is known for its biological properties and exhibits non-toxic effects besides being capable of undergoing biodegradation.[46]

Nguyen et al.[48] developed a nanogel called HP403, which is a combination of amphiphilic heparin and poloxamer P403. The researchers explored a nanogel that possesses the capacity to co-encapsulate cisplatin hydrate (CisOH) and curcuminoid (Cur) through distinct loading mechanisms. Comprehensive analysis of the HP403 nanogels and HP403@CisOH@Cur nanogels was conducted by the researchers using multiple techniques such as FT-IR spectroscopy, ^{1}H-NMR spectroscopy, DLS, and TEM. Through these analyses, it was established that the nanogels maintained their stability effectively and displayed a spherical structure. The drug release process indicated that Cur and CisOH were released at a faster rate under acidic conditions (pH 5.5) compared to under a neutral pH, thus affirming that the nanogels were effective in delivering the loaded compounds to tumor sites.

3.10. Gellan gum-based nanogels

Gellan gum, a type of polysaccharide, is recognized for its linear and negatively charged structure. The composition of the molecule includes a tetrasaccharide segment consisting of two β-D-glucose residues, one α-L-rhamnose residue, and one β-D-glucuronate residue.[80] These components make up ~60% glucose, 20% rhamnose, and 20% glucuronate. Gellan gum can be categorized into two types, high-acyl gellan gum, commonly known as native gellan gum, and low-acyl gellan gum, which is referred to as deacetylated gellan gum.

D'Arrigo et al.[49] created and characterized nanohydrogels that self-assemble using sonicated chains of gellan gum. They achieved this by chemically linking prednisolone (Pred), an anti-inflammatory drug with limited water solubility, to the carboxylic groups of gellan (Ge-Pred); Ge-Pred played a crucial role as the hydrophobic element accountable for the self-assembly mechanism. The researchers employed ^{1}H-NMR to analyze the Ge-Pred compound, while the cytotoxicity of Ge-Pred on cells was determined using the MTS assay. The self-aggregation characteristics of Ge-Pred in water were examined using the pyrene fluorescence technique, and the resulting nanohydrogels (NHs) were generated through bath sonication in an aqueous medium. Subsequently, these NHs were analyzed utilizing ζ-potential measurements and dynamic light scattering (DLS). The nanohydrogels exhibited an average size of ~300 nm and demonstrated negative ζ-potential values. The research findings demonstrated that Ge-Pred nanohydrogels were compatible with cells, facilitating the drug's bioavailability. As a result, these nanohydrogels present a promising and innovative carrier for delivering prednisolone.

10544 | *J. Mater. Chem. B*, 2023, **11**, 10538–10565

This journal is © The Royal Society of Chemistry 2023

3.11. Xanthan gum-based nanogels

Xanthan gum (XG) exhibits advantageous properties, including high solubility in water, remarkable biocompatibility, and substantial molecular weight. It is categorized as an *exo*-polysaccharide due to its structure consisting of branched polymeric chains.[81,82] In 1975, the fundamental composition of xanthan gum (XG) was determined, and its constituent units identified as pentasaccharides. XG is composed of D-glucosyl, D-mannosyl, and D-glucuronyl acid residues in a molar ratio of $2:2:1$. Additionally, it contains different amounts of pyruvyl and *O*-acetyl residues. Structurally, XG bears a close resemblance to cellulose, as it exhibits a linear arrangement of D-glucose units linked by (1–4) bonds.[83,84]

Ferreira *et al.*[85] conducted a study to investigate the potential anti-tumor effects of polymeric nanocapsules (NC (PhSe)$_2$) loaded with (PhSe)$_2$ on a melanoma cell line called SK-Mel-103, known for its resistance. Additionally, they developed a xanthan gum-based hydrogel for the topical application of NC (PhSe)$_2$. In the *in vitro* evaluation, the researchers exposed the cells to different concentrations (ranging from 0.7 to 200 μM) of either free (PhSe)$_2$ or NC (PhSe)$_2$. After 48 hours, they conducted the MTT assay to assess cell viability, measured propidium iodide uptake (a marker for necrosis), and evaluated nitrite levels. The hydrogels were prepared by incorporating xanthan gum into the suspension of NC (PhSe)$_2$ or the (PhSe)$_2$ solutions to increase their viscosity. The researchers conducted various characterization tests on the hydrogels, including determination of their average diameter, pH, polydispersity index, spreadability, drug content, and rheological profiles. Additionally, they evaluated the *in vitro* permeation of the hydrogels through human skin.

4. Different types of stimulus-responsive polysaccharide nanohydrogel

Nanohydrogels have emerged as promising candidates for delivering bioactive substances like drugs, genes, proteins, and enzymes in various drug delivery systems.[63] One area of particular interest is the development of stimuli-responsive polymeric nanoparticles, which can detect and respond to internal and external stimuli such as chemical, physical, and biological signals. These nanoparticles, often referred to as "smart" or "intelligent" biomaterials, are highly sought after for their ability to adapt to their surroundings and exhibit environmentally sensitive behavior.

4.1. pH-Responsive polysaccharide nanohydrogel

Extensive research has been focused on pH-responsive nanogels, particularly in the realm of targeted drug delivery systems for the treatment of cancer. One distinguishing feature of the tumor microenvironment (TM) is its acidic pH, which sets it apart from healthy tissue.[61] Within the tumor microenvironment (TM), both the extracellular and intracellular pH levels, including those in endosomes and lysosomes, exhibit noticeable acidity. The pH ranges for the extracellular environment and intracellular compartments are ~6.5–6.8 and 4.5–5.5,

respectively, in contrast to the normal physiological pH of 7.4. This acidic environment primarily arises from increased glucose conversion into lactic acid during glycolysis, providing additional energy for tumor cell survival. Exploiting this characteristic, pH-sensitive nanogels can be designed to enhance the effectiveness and efficiency of therapeutic interventions. Drug delivery systems that respond to changes in pH provide several benefits, including enhanced drug availability, improved cellular absorption, increased efficiency and stability of drug release, and targeted delivery to specific locations. Nanogels are often designed to exhibit pH responsiveness by incorporating ionizable groups, namely NH$_2$ and –COOH, into the constituent monomers or polymers. Alternatively, they may contain acid-sensitive linkages like ketal, acetal, and hydrazine, among other possibilities. The inclusion of acid-sensitive groups or linkages in nanogels leads to changes in their physicochemical properties. When exposed to an acidic environment, pH-responsive nanogels can swell as a result of electrostatic repulsion among the formed ions or undergo chain dissociation or degradation. These alterations enable the controlled release of drugs. Fig. 5 visually depicts the drug delivery mechanism utilizing acid-sensitive nanogels.[86]

The pH-responsive degradation of hydrogels is responsible for the targeted discharge of cargo. Zheng *et al.*[87] have developed a hybrid hydrogel that combines micelles and nanocomposites for applications in skin cancer treatment and bacterial extermination, both *in vitro* and *in vivo*. They designed a responsive hydrogel system that can respond to multiple stimuli, leading to enhanced photothermal and chemodynamic therapy (CDT). The hydrogel was created by incorporating MoS$_2$@MnFe$_2$O$_4$ nanocomposites into a cross-linked network consisting of chitosan-*grafted*-dihydrocaffeic acid (CS–DA) and aldehyde Pluronic F127 (F127-CHO) micelles laden with glucose oxidase (GOx). The hydrogel network contained dynamic Schiff-based imine bonds, which allowed for pH responsiveness and controlled degradation of the gel. The hydrogel exhibited a loading capacity of 0.5666 mg g^{-1} for GOx, and ~60% of GOx was released over 15 days under a slightly acidic pH of 6.8. Upon release, the GOx enzymatically reacted with glucose, resulting in the generation of hydrogen peroxide and increased acidity in the environment. This acidity allowed iron atoms to participate in the Fenton reaction, producing reactive hydroxyl radicals that induced cell death. The combination of chemodynamic therapy (CDT) with local hyperthermia effectively suppressed tumor growth, achieving a suppression rate of 98.8% *in vitro* and 97.6% *in vivo*.

pH-Responsive nanogels find extensive application in drug delivery, and they can be synthesized using both synthetic and natural polymers. Natural polymers like cellulose, chitosan, hyaluronic acid, and dextrin, among others, are highly preferred due to their favorable attributes such as biocompatibility, biodegradability, and non-toxic nature.

In a study conducted by Rahmani *et al.*,[88] a new nanocomposite was created using pH-responsive chitosan (CS), nitrogen-doped carbon quantum dots (NCQDs), and montmorillonite (MMT) (Fig. 6). This nanocomposite was loaded with doxorubicin (DOX) and introduced into a double emulsion system to

This journal is © The Royal Society of Chemistry 2023

J. Mater. Chem. B, 2023, **11**, 10538–10565 | **10545**
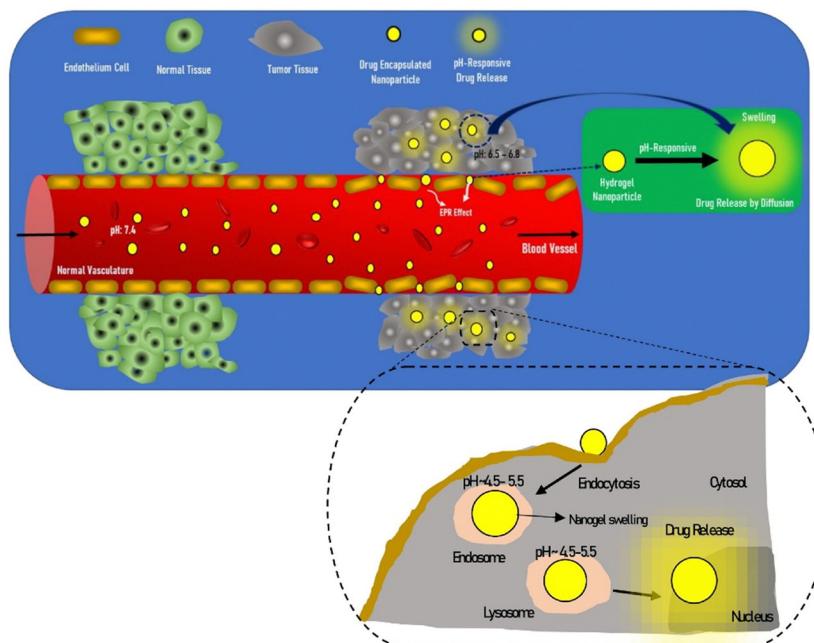
Fig. 5 The process of delivering drugs using acid-sensitive nanogels. Reproduced from ref. 86 with permission from Elsevier, copyright 2023.
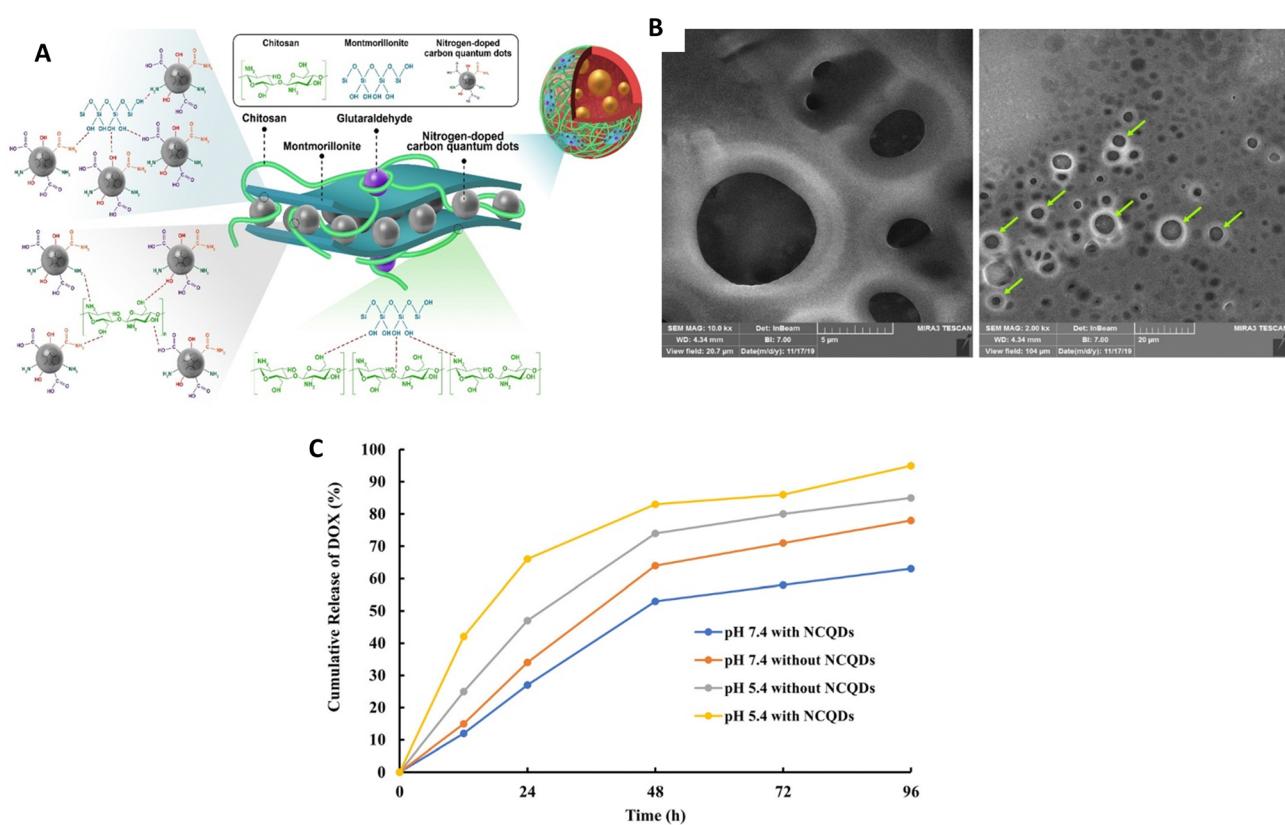

Fig. 6 (A) A structural depiction of a hydrogel nanocomposite consisting of cross-linked chitosan (CS), nanocrystalline quantum dots (NCQDs), montmorillonite (MMT) and the drug doxorubicin (DOX) shown as a diagram. (B) An image obtained through field-emission scanning electron microscopy (FESEM) showing the CS–MMT–NCQDs nanocarrier loaded with DOX. (C) The release pattern of DOX from the CS–MMT–NCQDs nanocarrier and CS–MMT without NCQDs *in vitro* at pH 5.4 and pH 7.4, both at 37 °C, using the dialysis protocol; release profiles measured at specific time intervals. Reproduced from ref. 88 with permission from Wiley, copyright 2022.

achieve a controlled and prolonged release of the drug. The incorporation of nitrogen-doped carbon quantum dots (NCQDs) into the CS–MMT hydrogel resulted in notable enhancements in loading and entrapment efficiencies. Additionally, the presence of NCQDs nanoparticles in the CS–MMT hydrogel enabled an extended and pH-responsive release of doxorubicin (DOX) for a duration of 96 hours, surpassing the release profile demonstrated by CS–MMT–DOX nanocarriers at pH 5.4. The release of DOX was precisely controlled and followed the Korsmeyer–Peppas model at pH 5.4, ensuring reduced side effects. On the other hand, no diffusion of DOX was observed at pH 7.4, indicating the potential to minimize the undesirable effects.

An alternative method of developing pH-responsive nanogels involves utilizing polymer components that contain amino functionalities, known as cationic polymers. These polymers have the ability to ionize (protonate) and form NH^{3+} when exposed to an acidic environment. This ionization process leads to enhanced electrostatic repulsion, triggering a volume-phase transition or swelling of the nanogels. The swelling phenomenon is of paramount importance in the controlled release and regulation of drugs. Furthermore, nanogels with a positive charge have a heightened affinity for negatively charged cell membranes, facilitating their rapid internalization by cells.

Rong *et al.* conducted a study,[89] deploying an injectable composite hydrogel that was obtained by combining hydroxypropyl chitosan (HPCS) and oxidized hyaluronic acid (OHA) through the formation of imine bonds (Fig. 7); functional substances could be delivered using this hydrogel. To enhance its properties, mesoporous polydopamine (MPDA) nanoparticles were integrated into the gel, serving both as an effective
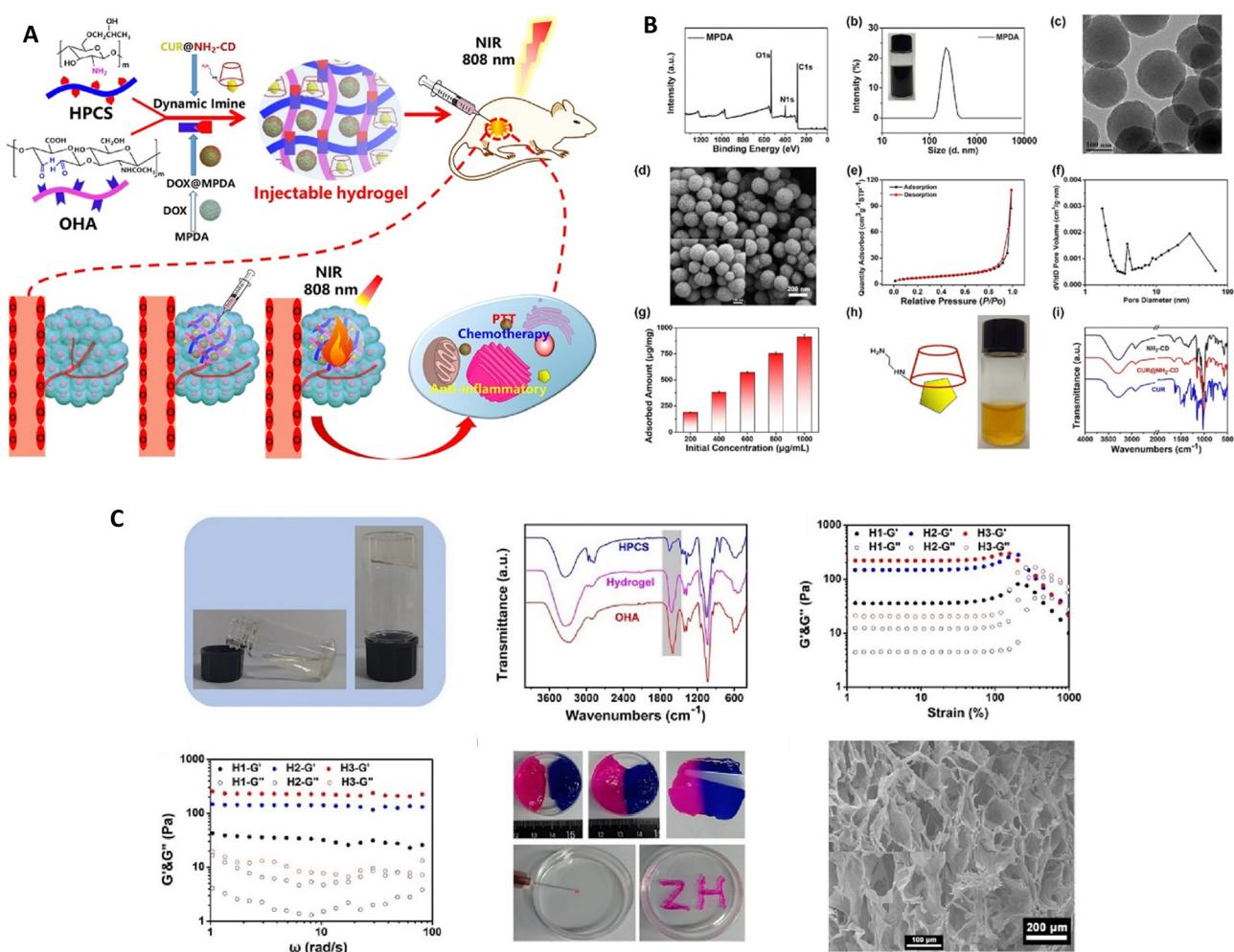

Fig. 7 (A) A diagram depicting the conceptual framework of the hydrogel composite intended for tumor treatment utilizing near-infrared (NIR) irradiation. (B) Various analyses were conducted to assess the characteristics of the materials, including the X-ray photoelectron spectroscopy (XPS) wide-scan spectrum, Fourier-transform infrared (FTIR) spectra, size distribution assessment, transmission electron microscopy (TEM) and scanning electron microscopy (SEM) images, nitrogen (N_2) sorption isotherm measurement, doxorubicin (DOX) adsorption capacity evaluation, and determination of the corresponding pore size distribution of the MPDA. (C) The process of gelation of the resultant hydrogel, the Fourier-transform infrared (FTIR) spectra of the hydroxypropyl cellulose sulfate (HPCS), octylphosphonic acid (OHA), and the respective hydrogel, the storage modulus (G') and loss modulus (G'') of the hydrogel with a gradient composition, as determined through strain sweep and frequency sweep experiments, the images showcasing the self-healing and injecting procedures of the hydrogel, and the scanning electron microscopy (SEM) images of the freeze-dried hydrogel. Reproduced from ref. 89 with permission from Elsevier, copyright 2023.

photothermal agent and a reservoir for the drug doxorubicin (DOX). This combination allows for effective photothermal conversion and controlled discharge of the drug. In addition, to tackle inflammation resulting from photothermal therapy (PTT), the scientists introduced the curcumin–cyclodextrin host–guest inclusion complex (CUR@NH$_2$-CD) into the hydrogel. *In vivo* experiments demonstrated that the composite hydrogel effectively inhibited the growth of Hepa1-6 tumors, benefiting from the synergistic effects of MPDA's photothermal properties, DOX's chemotherapy, and CUR's anti-inflammatory activity. These findings indicate that the composite hydrogel has significant potential for comprehensive tumor therapy.

4.2. Temperature-responsive polysaccharide nanohydrogel

Thermo-responsive polymeric nanoparticles have mainly been used for the precise and controlled delivery of drugs. The temperature in and around diseased areas tends to be higher than the normal body temperature. The distinct properties of tumors have spurred the advancement of temperature-responsive nanogels. At a distinct temperature referred to as the volume-phase transition temperature (VPTT), these nanogels undergo a volume-phase transition, which can manifest as either swelling or deswelling. This transition enables the controlled discharge of drugs within a targeted region. In some instances, external heat is applied to the target site using methods such as light irradiation, electric or magnetic fields, or external heating to trigger the release. Besides polymeric nanogels, nanocarriers based on liposomes, dendrimers, metal nanoparticles, and other materials have also been designed as temperature-responsive nanocarriers for targeted drug delivery.

The role of thermoresponsive nanogels as nanocarriers relies on the properties of responsive moieties/polymers, which exhibit a lower critical solution temperature (LCST). At temperatures below the LCST, nanogels maintain sufficient hydration in a water-based environment and form hydrogen bonds with water molecules. However, as the temperature rises above the LCST, nanogels undergo a volume-phase transition, becoming more hydrophobic. This results in the shrinkage of the nanogel structure, enabling the release of drug molecules. The transition is triggered by a reduction in the hydrophilic interactions between the polymer and water molecules, leading to an increase in intra- and inter-hydrophobic interactions among the polymer molecules. The precise lower critical solution temperature (LCST) of a thermosensitive polymer is dictated by its structure and composition, and it can be altered by manipulating the composition of the nanogel. Although PNiPAAm is frequently utilized in nanogel synthesis due to its LCST range of 30–35 °C, its potential toxicity and lack of biodegradability restrict its application as a nanocarrier. To overcome these limitations, efforts have been made to enhance the biodegradability and biocompatibility of nanogels by integrating copolymerization or grafting techniques with biodegradable polymers like cellulose, chitosan, hyaluronic acid, dextran, and similar materials.

Nanogels with temperature responsiveness, derived from hyaluronic acid (HA) and grafted with PNIPAM, have exhibited enhanced drug loading capacity and improved bioavailability when nanogels are utilized for curcumin, which is a hydrophobic anti-cancer medication. The synthesis of HA nanogels grafted with PNIPAM was accomplished using the sonification method, yielding nanogels with a narrow size distribution ranging from 100 to 300 nm and a polydispersity index (PDI) of 0.2. Premature dispensation of the drug payload prior to reaching the intended target sites is a significant challenge in drug delivery systems. To address this issue, the development of nanogels with a hollow-shell structure has been explored, which have the ability to efficiently uptake, store, and subsequently release the cargo, providing a solution to the aforementioned challenge.

Luckanagul *et al.*[90] have developed intelligent material platforms for the delivery of curcumin, *via* the deployment of nanoscale hydrogel particles derived from the natural polymer chitosan (Fig. 8). In this investigation, chitosan was employed as the fundamental material and subjected to a chemical grafting process with poly-(*N*-isopropylacrylamide) (pNIPAM) using an EDC/NHS coupling reaction. The resulting conjugated products were analyzed and characterized using TGA and ^{1}H NMR techniques. By employing a sonication method, chitosan-grafted pNIPAM (CS-*g*-pN) nanogels were prepared, and the loading of curcumin into these nanogels was accomplished
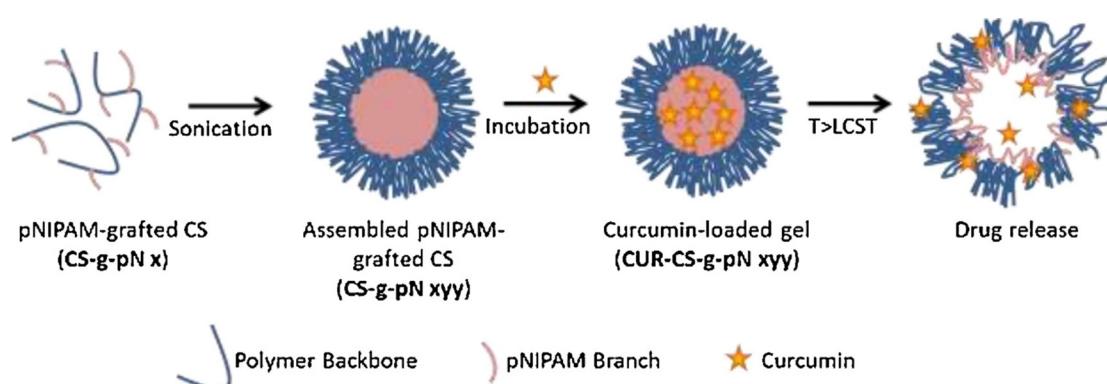

Fig. 8 The schematic representation of assembly and drug release of CS-*g*-pN nanogels. Reproduced from ref. 90 with permission from Elsevier, copyright 2018.

10548 | *J. Mater. Chem. B*, 2023, **11**, 10538–10565

This journal is © The Royal Society of Chemistry 2023
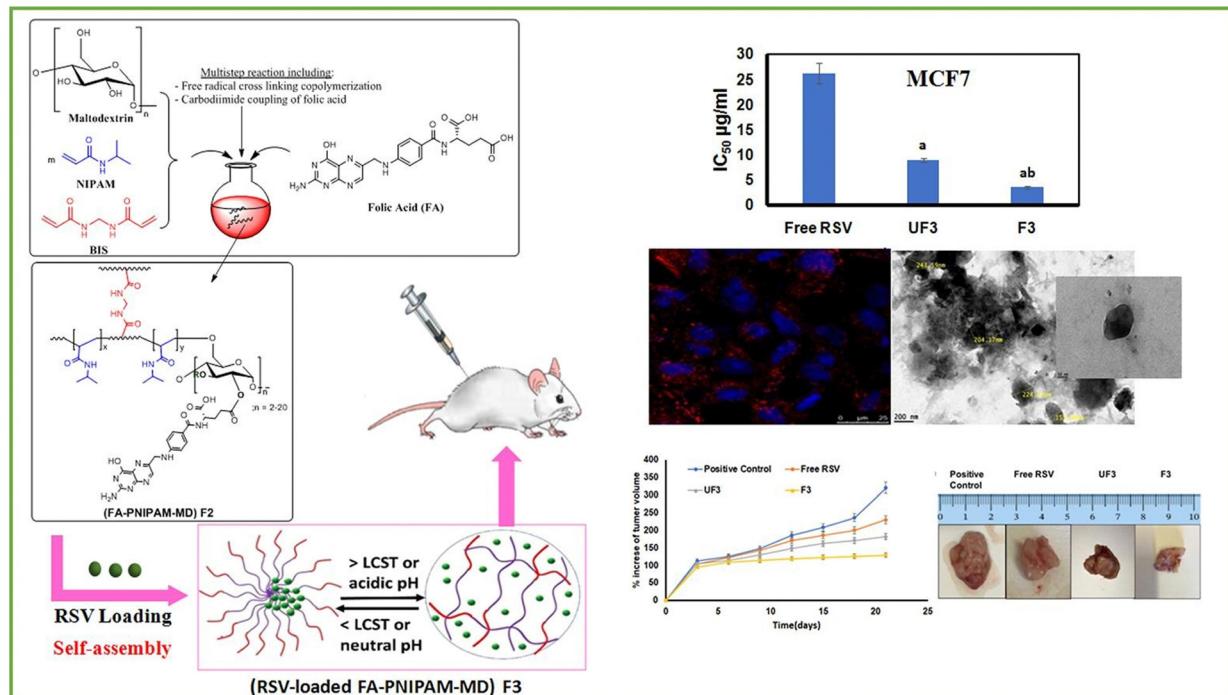
Fig. 9 An illustration of the novel thermo-/pH-responsive nanohydrogels composed of folic acid–poly(N-isopropylacrylamide–maltodextrin) for targeted therapy of breast cancer using resveratrol. Reproduced from ref. 91 with permission from Elsevier, copyright 2023.

through an incubation process. Various analytical techniques, including DLS, TEM, fluorescent spectroscopy, and confocal microscopy, were utilized to investigate the size, morphology, curcumin loading capacity, and cellular uptake of the nanogels, respectively. To evaluate the safety of the CS-g-pN nanogel particles, the CellTiter-Blue® cell viability assay was conducted on NIH-3T3 and HeLa cells. Additionally, an MTT assay was performed on HepG2, Caco-2, MDA-231, and HT-29 cells to assess the cytotoxic effects. The findings indicated that CS-g-pN nanogel particles with submicron sizes could be easily formed by assembling CS-g-pN with a modification degree ranging from 3% to 60%, and the resulting nanogels efficiently encapsulated curcumin. The thermoresponsive properties of the different CS-g-pN nanogel formulations varied based on the density and length of the grafted pNIPAM. Moreover, the CS-g-pN nanogel preparations displayed no toxicity towards HeLa cells or NIH-3T3. Each curcumin-loaded CS-g-pN nanogel formulation was taken up by NIH-3T3 cell lines and exhibited cytotoxicity against the tested cell lines in a dose-dependent manner.

Metawea and his colleagues[91] conducted research on the development of poly(N-isopropylacrylamide) (PNIPAM) due to its versatility for chemical modifications, allowing adjustment of its thermoresponsive properties and incorporation of additional stimulus responsiveness (Fig. 9). The main goal of this study was to create a delivery system for resveratrol (RSV), a natural polyphenol with limited bioavailability in breast cancer treatment, that is both targeted and responsive to stimuli. To achieve this, PNIPAM-maltodextrin nanohydrogels (PNIPAM-MD NGs) were synthesized and decorated with folic acid (FA).

4.3. Enzyme-responsive polysaccharide nanohydrogel

Enzymes, which are crucial proteins in the human body, play a significant role in facilitating chemical reactions and have great promise for enhancing drug release. They can also accelerate the formation of specific substances, like acids, that can initiate the discharge of drugs. In controlled drug transport, specific enzymes that are found in high levels in tumor cells or the tumor microenvironment can trigger the release of drugs. These enzymes include cathepsin B, MMP-2, MMP-9, and NAD(P)H: quinone oxidoreductase1, among others.

Yang et al.[92] developed methacrylated hyaluronic acid (HA) nanogels that respond to enzymes for delivering anti-cancer drugs (DOX) to various cancer cells, like NIH3T3, A549, and H22 (Fig. 10). The HA nanogels were synthesized using radical copolymerization with the incorporation of a crosslinker called di(ethylene glycol) diacrylate (DEGDA), which contained enzyme-cleavable ester bonds. The researchers observed the disintegration or breakdown of the enzyme-sensitive nanogel networks by monitoring the change in light scattering intensity (I_t/I_0) of the HA nanogels when exposed to hyaluronidase (Haase) and lipase enzymes. This demonstrated that the nanogels could respond to specific enzymes. The researchers conducted evaluations of the nanogels both in vitro and in vivo to assess their suitability for drug delivery applications.

Gao et al.[93] created a specific nanogel system for treating breast cancer by combining CD44 and biotin receptors, wherein they were loaded with paclitaxel (PTX/Bio-NG). After fabrication using enzyme-sensitive hyaluronic acid, nanogels exhibited a spherical shape with an average particle size of 149.1 ± 1.6 nm (Fig. 11). They demonstrated high entrapment efficiency
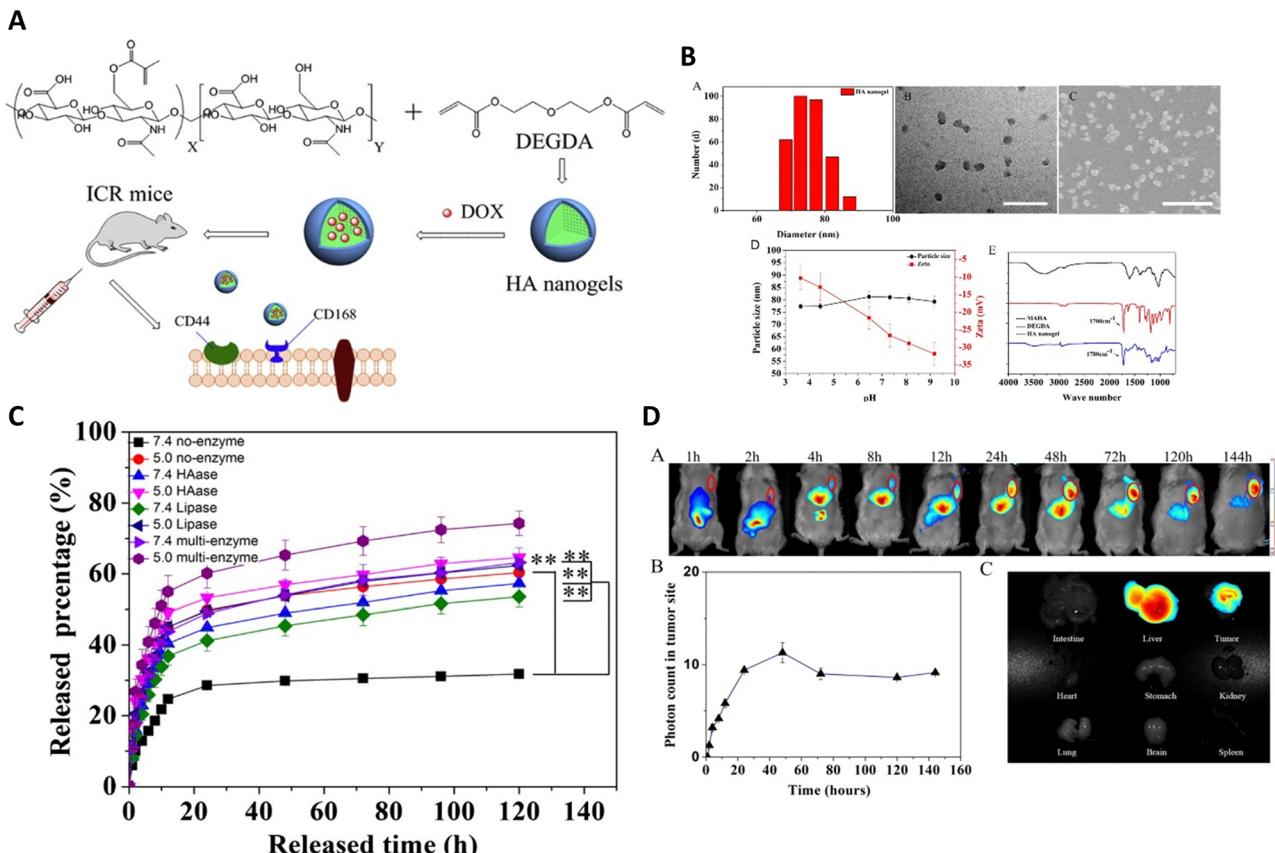
Fig. 10 (A) The synthesis pathway for producing HA nanogels is depicted. (B) The hydrodynamic diameter distribution of the HA nanogels is performed using DLS, TEM and SEM images of the HA nanogels, scale bar representing 200 nm with the impact of pH on the particle size and zeta potential of the HA nanogels. The FT-IR spectrum illustrates the comparison between MAHA (black), DEGDA (red), and the HA nanogels (blue). (C) The *in vitro* release profiles of DOX from the nanogels are evaluated in PBS at pH 5.0 and pH 7.4, at 37 °C, with and without hyaluronidase, lipase, and two other enzymes, respectively. (D) *In vivo* near-infrared (NIR) fluorescence imaging of H22 tumor-bearing mice after intravenous injection of NIR-797 labeled HA nanogels, and NIR fluorescence intensity of the tumor being measured at different time intervals in mice treated with HA nanogels. Reproduced from ref. 92 with permission from Elsevier, copyright 2015.

(90.17 ± 0.52%) and drug loading (15.28± 0.10%). When exposed to hyaluronidase and/or lipase enzymes, the PTX/Bio-NG formulation displayed rapid drug release. Cellular studies verified that the internalization of Bio-NG by 4T1 cells occurred *via* both the CD44 receptor and the biotin-specific receptor. PTX/Bio-NG, in comparison to PTX-loaded nanogels lacking biotin (PTX/NG), exhibited improved cytotoxicity against breast cancer cells (4T1 cells). Pharmacokinetic analysis conducted in rats demonstrated higher AUC0-t values and lower clearance rates for PTX/NG (6.24 times and 15.96%, respectively) as well as PTX/Bio-NG (6.66 times and 14.89%, respectively) when compared to the control group (Taxol). *In vivo* studies performed on Balb/c mice with 4T1 tumors demonstrated the excellent therapeutic efficacy of PTX/Bio-NG, indicating its potential as a promising candidate for breast cancer treatment.

4.4. Glucose-responsive polysaccharide nanohydrogel

Various forms of glucose-responsive hydrogels can be utilized,[1,94] including microgels,[95] nanogels,[96] microneedles,[97–99] micelles,[100] and mesoporous nanoparticles, which offer diverse options for the application of glucose-responsive nanogels, allowing for flexibility in their use.

El Shaarani *et al.*[96] performed a study involving the synthesis of various glucose-responsive nanogels using 4-(1,6-dioxo-2,5-diaza-7-oxamyl) phenylboronic acid (DDOPBA) and N-isopropylacrylamide (NIPAM) (Fig. 12). To serve as the crosslinker, they employed dextran-grafted maleic acid (Dex-MA). The nanogels, referred to as P(NIPAM-co-Dex-co-DDOPBA)s, underwent characterization through various methods, including DLS, TEM, 1H NMR, and X-ray photoelectron spectroscopy (XPS). The incorporation of DDOPBA, which contains an electron-withdrawing group, resulted in significant sensitivity to glucose at physiological pH due to its unique properties. Furthermore, the hydrophilic Dex-MA played a role in modulating the temperature sensitivity of the nanogels near physiological temperatures. The nanogels demonstrated excellent capacity for insulin loading and exhibited a high encapsulation efficiency. In *in vitro* experiments, the release of insulin from the loaded system was found to be contingent on the concentration of glucose under physiological pH and temperature conditions. This glucose-dependent response allowed for controlled insulin release based on glucose levels. Overall, the study successfully synthesized and characterized glucose-responsive nanogels with desirable properties for drug delivery applications.

10550 | *J. Mater. Chem. B*, 2023, **11**, 10538–10565

This journal is © The Royal Society of Chemistry 2023
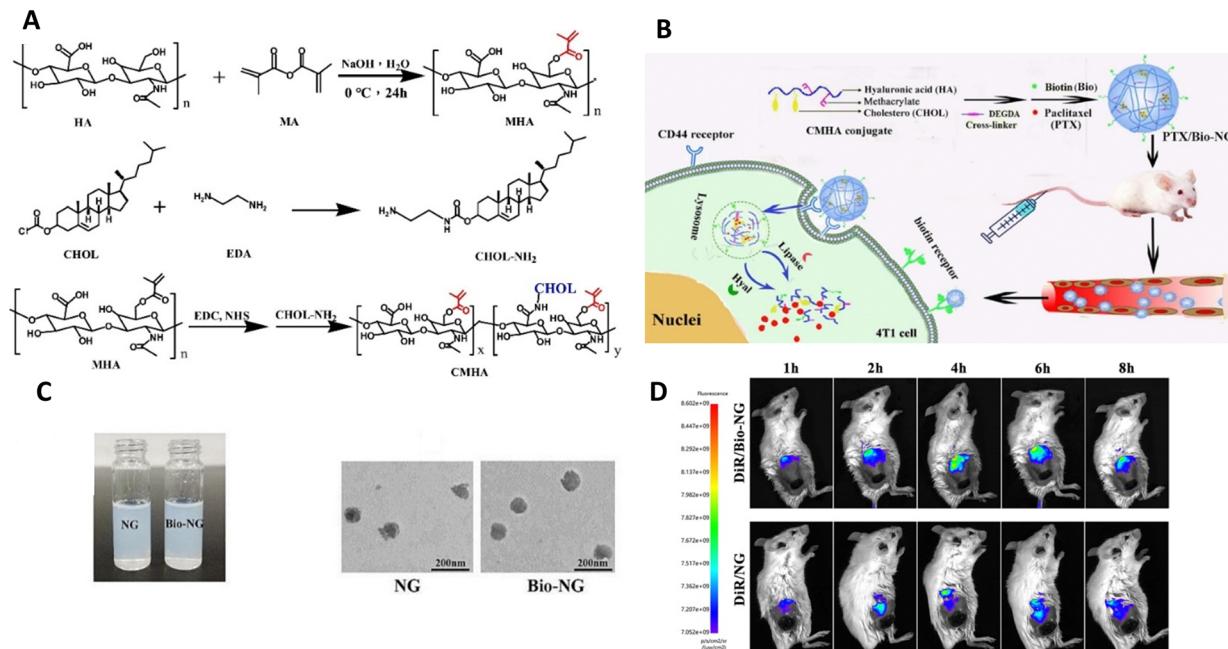
Fig. 11 (A) Synthetic schemes for MHA, CHOL–NH₂, and CMHA. (B) Schematic illustration showcasing the preparation of PTX/Bio-NG and its *in vivo* drug transport process. (C) The appearance of PTX/NG and PTX/Bio-NG, along with a TEM image of PTX/NG. (D) Performing in vivo imaging on 4T1 tumor-bearing mice using DiR-loaded formulations. Reproduced from ref. 93 with permission from Elsevier, copyright 2022.

Zhang *et al.*[42] developed a novel therapeutic strategy, involving lactoferrin (Lf) and phenylboronic acid (PBA)-functionalized hyaluronic acid nanogels for the treatment of glioma (Fig. 13), and the nanogels were crosslinked using a disulfide-bond cross-linker. This platform, referred to as Lf-DOX/PBNG, is specifically designed to deliver doxorubicin hydrochloride (DOX). The spherical Lf-DOX/PBNG nanogels are endowed with optimized physicochemical properties and exhibit rapid release of DOX under high concentrations of glutathione, which serves as a reduction-sensitive trigger. In cellular investigations, Lf-DOX/

PBNG demonstrated enhanced cytotoxicity, increased cellular uptake efficiency, and significantly improved permeability in the brain when compared to neat DOX solution, DOX-loaded PBA functionalized nanogels (DOX/PBNG), and Lf-modified DOX-loaded nanogels (Lf-DOX/NG). Pharmacokinetic analysis indicated that the area under the curve for DOX/PBNG, Lf-DOX/NG, and Lf-DOX/PBNG increased by 8.12, 4.20, and 4.32 times, respectively, in comparison to the DOX solution. Biodistribution studies confirmed that Lf-DOX/PBNG accumulated in the brain at levels 12.37 and 4.67 times higher than neat DOX
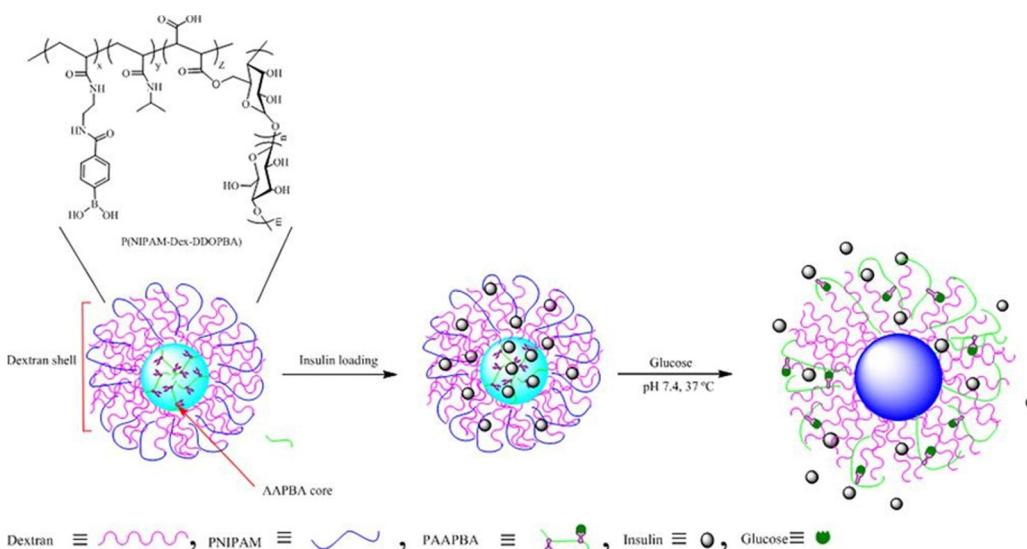
**Fig. 12** Schematic illustration of glucose-responsive nanogel. Reproduced from ref. 96 with permission from Elsevier, copyright 2020.

This journal is © The Royal Society of Chemistry 2023

*J. Mater. Chem. B*, 2023, **11**, 10538–10565 | **10551**

Fig. 13 A schematic illustration of Lf-DOX/PBNG for improving BBB penetration and glioma targeting of DOX through receptor-mediated endocytosis. Reproduced from ref. 42 with permission from Elsevier, copyright 2022.

solution and DOX/PBNG, respectively. These findings emphasize the potential of Lf-DOX/PBNG as an exceptionally effective targeting system for glioma therapy.

4.5. Light-responsive polysaccharide nanohydrogel

The use of light irradiation encompasses the act of subjecting a sample to light with a specific wavelength, a process that can be readily accomplished. Employing light as a stimulus initiator offers the benefit of toggle-like functionality, enabling precise management of the duration of exposure for a specific system.

Extensive research has been conducted on nanoparticles and nanogels that respond to light, during the exploration of their potential applications in targeted drug delivery, diagnostics, and monitoring the progress of healing. These nanocarriers, being sensitive to light, facilitate the transportation of drugs to specific locations through passive, active, and internalization mechanisms. Phototherapy commonly utilizes ultraviolet (UV), visible, and near-infrared (NIR) light. UV light, with a wavelength range of 100–380 nm, has been widely researched for its ability to trigger drug release due to its high sensitivity and energy, which can induce structural changes in materials. However, UV light has limitations such as poor tissue penetrability and phototoxicity, which restrict its use in biomedical applications. On the contrary, visible and infrared lights possess an enhanced capability to penetrate deep tissues as they experience minimal attenuation. The material's reaction to light is contingent upon various factors, including wavelength, intensity/energy, polarity, and length of exposure. While near-infrared light offers advantages in terms of tissue penetration, its limited energy hampers its efficacy in drug transport systems.

The use of light as a trigger for drug transport offers several benefits, including non-invasiveness, precise control over

timing and location, and user-friendliness. Nanogels, whether they contain or are attached to bioactive substances or therapeutic medications, experience physical or structural modifications upon exposure to light. These changes enable the targeted discharge of the drug at a specific location. In drug delivery systems activated by light, three main categories of changes in physical, chemical, or structural properties play a crucial role: (i) photochemical alterations, which involve the oxidation, cleavage of bonds, and photopolymerization; (ii) photoisomerization; and (iii) photothermal variations. These modifications in the nanocarriers enable precise and controlled release of the drug when exposed to light stimuli.

Degradable nanogels with the ability to respond to ultraviolet (UV) light and near-infrared (NIR) light have been developed by Hang et al.[101] These nanogels utilize hyaluronic acid-*g*-7-*N,N*-diethylamino-4-hydroxymethylcoumarin (HA-CM) and are specifically designed for targeted intracellular delivery of doxorubicin (DOX) through CD44 receptors, offering remote control over the drug discharge (Fig. 14). The nanogels, which are of nanometer size, efficiently encapsulate DOX. The nanogels' response to NIR or UV light leads to a significant increase in the release of DOX. This effect is caused by the light-induced breakdown of the urethane bonds that connect CM to HA. When DOX-loaded HA-CM nanogels are combined with NIR irradiation in MTT assays, they exhibit impressive antitumor activity against MCF-7 cells (CD44+), surpassing the activity against U-87MG cells (CD44−) and free HA-pretreated MCF-7 cells. The uptake of DOX-loaded HA-CM nanogels by CD44+ cells was confirmed through observations made using confocal laser scanning microscopy (CLSM). The uptake process occurs *via* receptor-mediated endocytosis, and the release of DOX inside the cells is induced by NIR light. These HA-CM nanogels possess favorable characteristics for cancer chemotherapy,
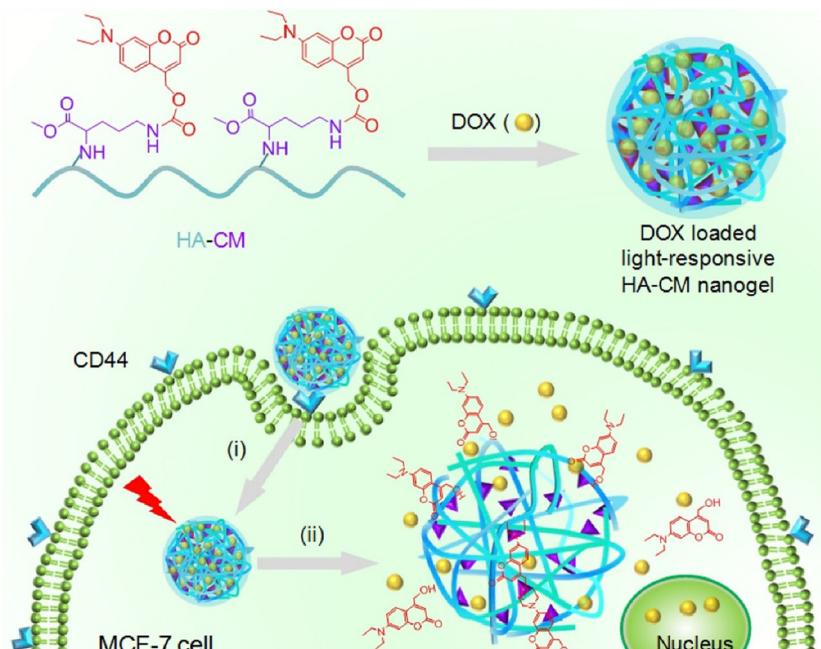
Fig. 14 Light-sensitive HA-CM nanogels for CD44 targeted and remotely regulated DOX discharge. (i) Receptor-mediated endocytosis and (ii) nanogel swelling and drug discharge upon exposure to light irradiation. Reproduced from ref. 101 with permission from Elsevier, copyright 2017.

such as easy preparation, targeting ability for CD44, and light-controlled release of the drug within cells.

4.6. Magnetic-responsive polysaccharide nanohydrogel

Generally, different types of magnetic nanomaterials, such as iron oxide (Fe_3O_4, γ-Fe_2O_3), transition metal ferrites ($CoFe_2O_4$, $MnFe_2O_4$, etc.),[102,103] and transition metal alloys (FePt), can be incorporated into nanogels as magnetic-responsive elements, thus allowing the creation of magnetic hydrogels suitable for biomedical purposes. However, among these potential nanoparticles, Fe_3O_4 nanoparticles have garnered significant interest and are extensively utilized in biomedical and pharmaceutical fields.[104,105] These characteristics contribute to the popularity of superparamagnetic iron oxide nanoparticles (SPIONs), which possess excellent biocompatibility, a high capacity for magnetization, and are relatively easy to prepare and functionalize. They have extensive usage across multiple domains such as magnetic resonance imaging (MRI), blood purification, drug administration, magnetic hyperthermia, in vivo biomarker identification, and cell patterning. In contrast to conventional magnetic particles, SPIONs do not retain their magnetic properties when the external magnetic field is removed. Rather, the magnetic nanoparticles within SPIONs react to variations in a magnetic field, producing heat that plays a vital role in ensuring efficient drug discharge.[106] The harmfulness of these nanoparticles is affected by various aspects like their dimensions, form, composition, and surface characteristics. Employing a concentrated magnetic field, magnetically sensitive nanocarriers can be introduced into solid cancer masses to improve the concentration of drugs specifically at the tumor locations.

Gao et al.[107] have developed a novel type of degradable nanogel known as polymer/Fe_3O_4 nanocomposite nanogels (NCGs), which possess magnetic, temperature-responsive, and redox-responsive attributes. To produce these NCGs, scientists modified the surface of Fe_3O_4 magnetic nanoparticles (MNPs) by introducing vinyl groups using 2-isocyanatoethyl methacrylate. Through a process called inverse miniemulsion polymerization, the NCGs were created using poly(N-vinylcaprolactam) (PNVCL) and Fe_3O_4, employing a cross-linker that contained disulfide. By chemically attaching the Fe_3O_4 MNPs to the polymer matrix, the structural integrity of the NCGs in water-based environments was ensured. The PNVCL/Fe_3O_4 NCGs possessed the desirable superparamagnetic properties of Fe_3O_4 MNPs and demonstrated reversible sensitivity to temperature changes as well as significant responsiveness to redox conditions. The release of a model anticancer drug, 5-fluorouracil, from the PNVCL/Fe_3O_4 NCGs could be suitably controlled by adjusting the external temperature, the redox state of the surrounding medium, or a combination of both. Moreover, the prepared PNVCL/Fe_3O_4 NCGs exhibited minimal cytotoxicity, suggesting their potential use as magnetic-guided nanocarriers for precise drug discharge (Fig. 15).

DNA nanogels have gained traction as miniature drug carriers in the field of biomedicine and pharmaceuticals due to their exceptional attributes such as biodegradability, biocompatibility, customizable sequence design, and tuning in size.[86] The negatively charged nature of DNA facilitates a strong interaction with positively charged drugs like doxorubicin, a potent anticancer medication. This interaction enhances the drug-loading capacity and effectiveness of DNA nanogels.[108–111] Recently, Yao et al.,[112] devised magnetic nanogels featuring a DNA nanogel shell-core structure incorporating iron oxide (Fe_2O_4), enabling targeted and triggered release of doxorubicin (DOX) in response to a magnetic field. The magnetic DNA nanogels (M-DNA) with a shell-core structure were created by first generating the DNA shell through a

This journal is © The Royal Society of Chemistry 2023

J. Mater. Chem. B, 2023, 11, 10538–10565 | 10553
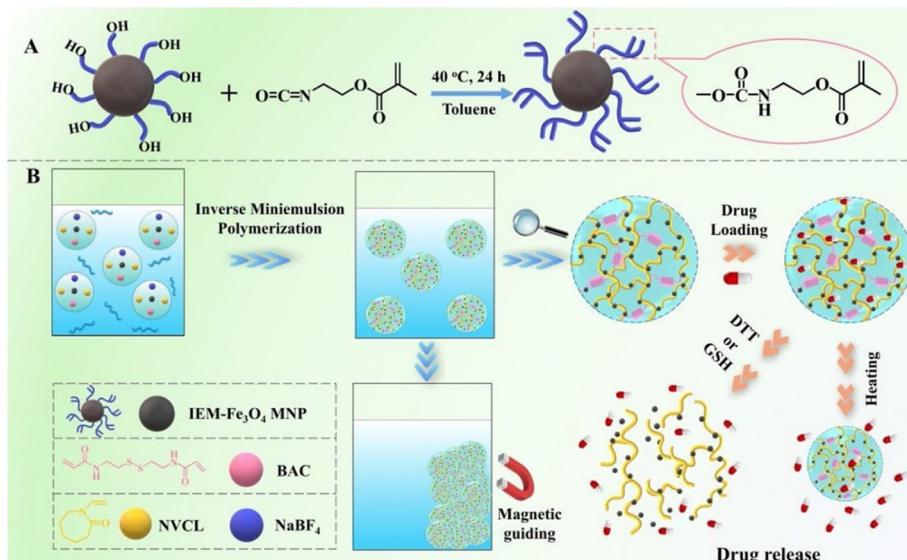
Fig. 15 (A) Synthesis process for the surface modification of Fe$_3$O$_4$ magnetic nanoparticles (MNPs) using IEM. (B) Schematic representation of the preparation, multi-responsiveness, as well as the loading and discharge actions of PNVCL/Fe$_3$O$_4$ nanocomposite nanogels (NCGs). Reproduced from ref. 107 with permission from Elsevier, copyright 2020.

process called rolling circle amplification (RCA), which is an enzymatic DNA polymerization (depicted in Fig. 16A). Subsequently, this DNA shell was coated onto the surface of Fe$_2$O$_4$ nanoparticles modified with amino groups (shown in Fig. 16B). The M-DNA nanogels would accumulate at the tumor site under the influence of an external magnetic field and release the drug in response to pH, temperature, and nuclease as triggers (illustrated in Fig. 16C). Scanning electron microscopy (SEM) imaging revealed the rough surface of the DNA polymer coating on Fe$_2$O$_4$ (shown in Fig. 16D). These meticulously prepared M-DNA nanogels exhibit responsiveness to multiple stimuli, releasing DOX in higher amounts with increasing temperature at pH 7.4 (Fig. 16E) and at lower pH levels (indicating acid sensitivity) (Fig. 16F). Moreover, the application of a magnetic field facilitates the penetration and accumulation of M-DNA nanogels (labeled in green with FTIC) into the tumor, demonstrating enhanced nanoparticle uptake and subsequent release of DOX (in red) into the cytoplasm and nucleus (in blue). This phenomenon becomes more prominent with increased incubation time of nanogels with U87MG cells (as evidenced in Fig. 16G).

4.7. Ultrasound-responsive polysaccharide nanohydrogel

Ultrasounds are produced by applying alternating current and are characterized by high frequency waves. They generate both thermal effects, causing a temperature increase, and non-thermal effects, *via* the formation of small gas bubbles. The formation and subsequent collapse of these bubbles can locally increase pressure and temperature, leading to changes in the mechanical attributes of the material. Additionally, ultrasounds have the capability to disassemble small vesicles like micelles or nanocarriers, which enables the efficient release of cargo substances, including anti-cancer drugs. However, polymer-based materials that respond to ultrasound are frequently utilized in various applications. These materials encompass polymer-coated bubbles and emulsions,[113] such as microbubbles, nanobubbles,[114]

nanodroplets,[115] and nanoemulsions.[116] Additionally, polymer vesicles or micelles[117] and polymer hydrogels[118] are commonly employed. These ultrasound-responsive drug delivery vehicles facilitate the delivery of diverse drugs, including small drug molecules, proteins,[119] and DNA.[120]

Maghsoudinia *et al.*[121] investigated the capabilities of theranostic nanoparticles made up of Gd-DOTA/doxorubicin-loaded perfluorohexane (PFH) nanodroplets for both drug delivery and imaging in B16F10 melanoma cancer cells. The internalization of sonicated Gd-DOTA/DOX@PFH nanodroplets by cancer cells was evaluated using inductively coupled plasma optical emission spectrometry (ICP-OES). The analysis indicated a 1.5-fold increase in uptake compared to non-sonicated nanodroplets after a 12 hour period. The biocompatibility of the synthesized nanodroplets was confirmed through *in vitro* and *in vivo* toxicity assays, which indicated the absence of organ toxicity. The application of ultrasound notably increased the release of doxorubicin from the nanodroplets, which exhibited strong ultrasound signal intensity and high r_1 relaxivity (6.34 mM^{-1} S^{-1}) for ultrasound echogenicity and T1-MRI relaxometry. The concentration of doxorubicin in the vital organs of mice was significantly lower for Gd-DOTA/DOX nanodroplets compared to free doxorubicin. In the Gd-NDs + US group, which was loaded with doxorubicin, the concentration of doxorubicin in the tumor region reached 14.8 µg g^{-1} after 150 minutes of sonication, representing a 2.3-fold increase compared to the non-sonicated group. These results emphasize the remarkable diagnostic capabilities (ultrasound/MRI) and therapeutic potential of the synthesized nanodroplets, positioning them as promising theranostic agents for targeted drug discharge in chemotherapy and cancer imaging.

4.8. Redox-responsive polysaccharide nanohydrogel

Apart from the established pH-triggered systems employed in drug delivery, novel strategies utilizing redox-triggered release

10554 | *J. Mater. Chem. B*, 2023, **11**, 10538–10565

This journal is © The Royal Society of Chemistry 2023
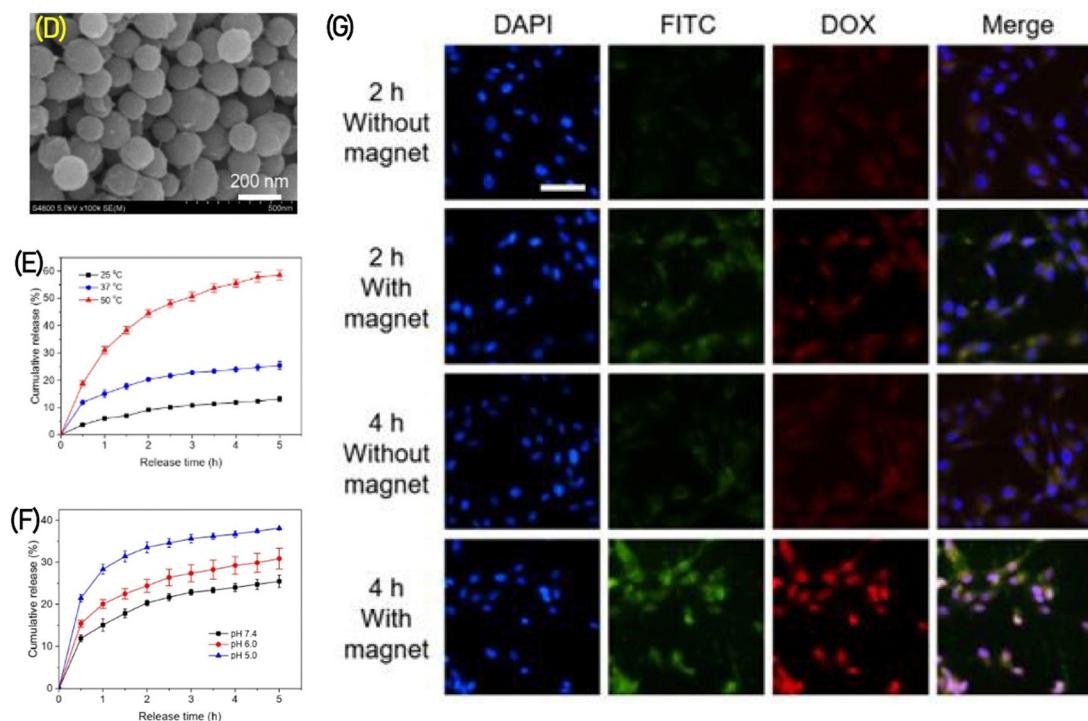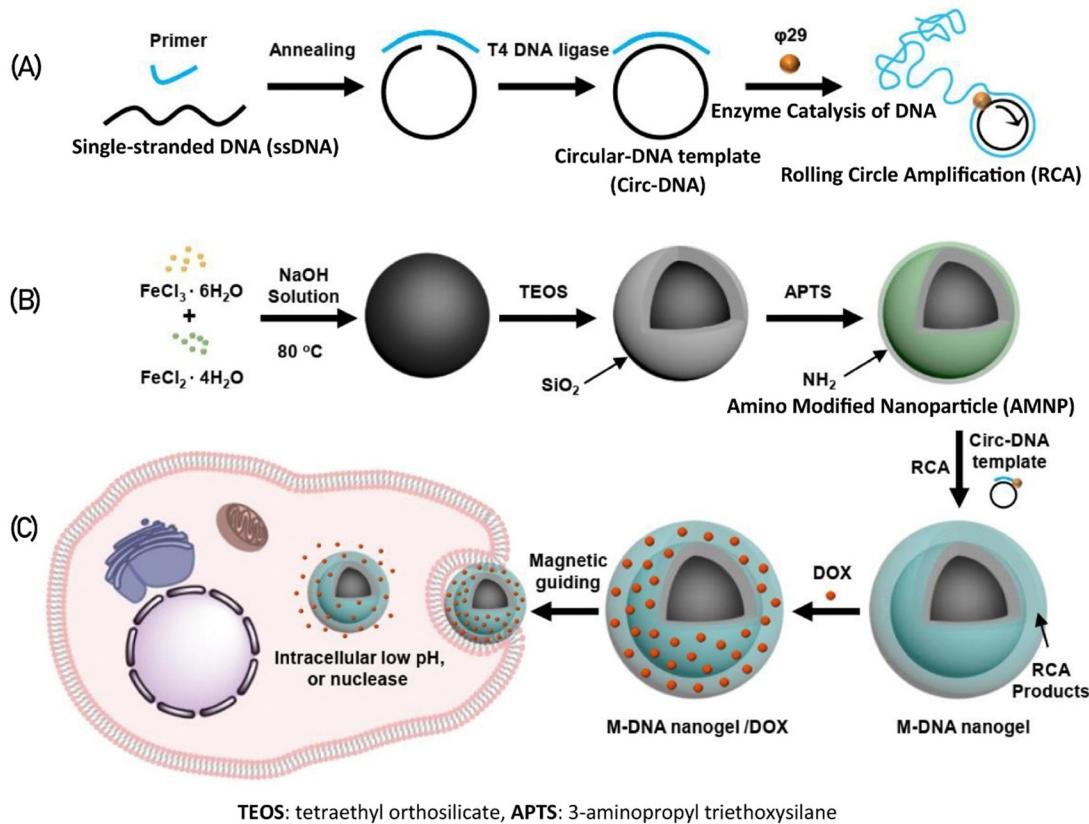
Fig. 16 illustrates the production process of M-DNA nanogels. (A) In the first step, a circular DNA template (circ-DNA) is created and subjected to rolling circle amplification (RCA). (B) Concurrently, amino-modified Fe_2O_4 nanoparticles are prepared. (C) These nanogels are designed to release DOX drug upon exposure to a magnetic field within tumor cells. (D) The SEM image portrays the structure of M-DNA nanogels. The release of DOX from M-DNA nanogels is showcased under various stimuli, including (E) different temperatures at pH 7.4 and (F) different pH levels at 37 °C. (G) Cellular uptake of FITC-stained M-DNA nanogels carrying DOX (depicted in blue) is observed in fluorescence images after incubation with U87MG cells for varying durations of 1, 3, 6, 12, and 14 hours. Reproduced from ref. 112 with permission from ACS, copyright 2022.

This journal is © The Royal Society of Chemistry 2023

J. Mater. Chem. B, 2023, **11**, 10538–10565 | **10555**

mechanisms have been developed to achieve targeted drug delivery. The existence of a redox gradient between the intracellular environment with reducing properties and the extracellular environment with oxidizing properties within a tumor serves as the basis for redox-sensitive nanogels.[122,123] The capability to regulate and direct drug delivery has attracted significant interest in nanogels as well as other polymeric nanoparticles like micelles, liposomes, and dendrimers. The intracellular microenvironments of cancer cells, comprising the cytoplasm, endosomes, and lysosomes, are characterized by elevated levels of glutathione (GSH), which creates a conducive reducing environment for redox-sensitive nanogels. The variance in redox potential between tumor cells and normal cells offers an ideal stimulus to induce physiochemical alterations in the nanogel's structure, thereby ensuring controlled drug delivery. To impart redox sensitivity, nanogels typically incorporate reduction-sensitive linkages. One frequently utilized linkage among these connections is the disulfide (–S–S–) bond, which can be reduced to thiols (–SH) in reductive environments such as the cancer microenvironment rich in glutathione (GSH). The breakdown of disulfide bonds in nanogels, which are typically stable in extracellular environments, allows for the controlled release of the active drug. Cleavable disulfide linkages in nanogels are attained by deploying crosslinkers bearing disulfide bonds, such as cystamine or dithiodipropionic acid, or through the polymerization of monomers containing disulfides.[124]

Degirmenci *et al.*[125] have developed a method for creating a modular nanogel system that responds to changes in oxidation

and reduction and was created by self-assembling dextran-based polymers through host–guest interactions. Nanogel construction involved the intentional utilization of the self-assembly process in a water-based environment, utilizing adamantane (Ada) and β-cyclodextrin (β-CD). By capitalizing on the particular host–guest interactions between β-cyclodextrin (β-CD) and adamantane (Ada), the nanogels were formed through the natural assembly of these molecular constituents. This self-assembly process allowed the fabrication of stable and well-defined nanogels with the desired properties and functionalities. Importantly, they deployed a crosslinker containing disulfide and bis-adamantane, which allowed the nanogels to degrade in response to glutathione (GSH), a naturally occurring reducing agent. In their experiments, the researchers also investigated the potential of loading doxorubicin (DOX) into these nanogels and combining them with a cyclic peptide-based targeting component that contains adamantane, allowing for a non-covalent interaction. Various *in vitro* studies were performed, focusing on drug release, cytotoxicity, and cellular internalization. The results demonstrated that the nanogels exhibited an enhanced release of the drug in an acidic and glutathione (GSH)-rich environment. Although the empty nanogels demonstrated no toxicity towards cells, the nanogels containing the drug displayed cytotoxic effects against MDA-MB-231 breast cancer cells. The highest level of cytotoxicity was observed in cells with elevated GSH levels when targeted with the drug-loaded nanogels incorporating the targeting component (Fig. 17).

Eskandani *et al.*[126] developed a magnetic hydrogel termed FSRMH, which is a stimuli-responsive system conjugated with
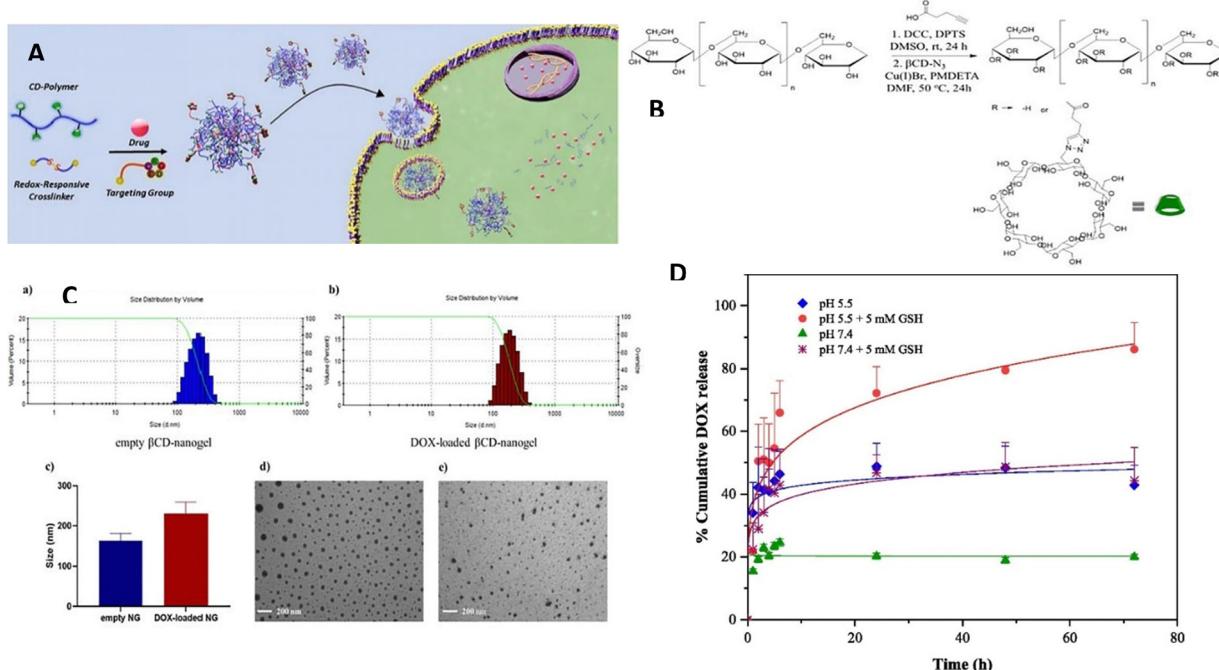


Fig. 17   (A) A diagram demonstrating the production process of targeted nanogels containing drugs. (B) The procedure for synthesizing βCD-Dex copolymer using a synthetic route. (C) The range of sizes observed in empty and DOX-loaded βCD-nanogels. (D) The release of DOX in a laboratory setting under different conditions: at pH 5.4 with and without GSH (5 mM), and at pH 7.4 with and without GSH (5 mM). Reproduced from ref. 125 with permission from Elsevier, copyright 2022.

10556 | *J. Mater. Chem. B*, 2023, **11**, 10538–10565

This journal is © The Royal Society of Chemistry 2023

folate (FA). This hydrogel has the capability to respond to changes in pH and redox conditions. The researchers utilized tragacanth gum (TG) as the main material for constructing the hydrogel, with the objective of employing it in chemo/hyperthermia therapy of MCF7 cells; the anti-cancer drug doxorubicin hydrochloride (Dox) was loaded into the FSRMH. The hydrogel's porous structure, along with strong hydrogen bonding and ionic interactions between its functional groups and the drug, facilitated efficient drug loading (LE; $8.1 \pm 0.25\%$) and encapsulation (EE; $81 \pm 2.50\%$). *In vitro* studies on drug release demonstrated that the FSRMH/Dox system exhibited minimal drug release under physiological conditions but displayed pH- and redox-triggered drug release behavior in cancerous conditions characterized by lower pH and higher glutathione (GSH) concentrations (Fig. 18). The biocompatibility of FSRMH was confirmed through an MTT assay, which indicated its cytocompatibility. Hemocompatibility assessment revealed that FSRMH had a hemolysis rate of $2.4 \pm 0.17\%$ at 100 μg mL^{-1}, thus affirming the safety of the

drug delivery system (DDS). Moreover, the DDS demonstrated a protein adsorption capacity of 59.6 ± 1.70 mg g^{-1}. The cytotoxicity of FSRMH/Dox was evaluated against MCF7 cells through an MTT assay, revealing a synergistic effect between chemotherapy and hyperthermia therapy, with a combination index (CI) of 0.609.

4.9. Electrical-responsive polysaccharide nanohydrogel

Among all the external stimuli available, an electric field stands out as a convenient and manageable option, particularly in the human microenvironment. Nanogels that respond to electrical stimulation, causing changes in their volume or shape, are typically composed of polyelectrolytes. These electro-responsive nanogels have the ability to convert electrical energy into mechanical energy. Consequently, they find applications as energy conversion devices in assorted fields such as robotics, sensors, controlled drug release systems, and artificial muscles.
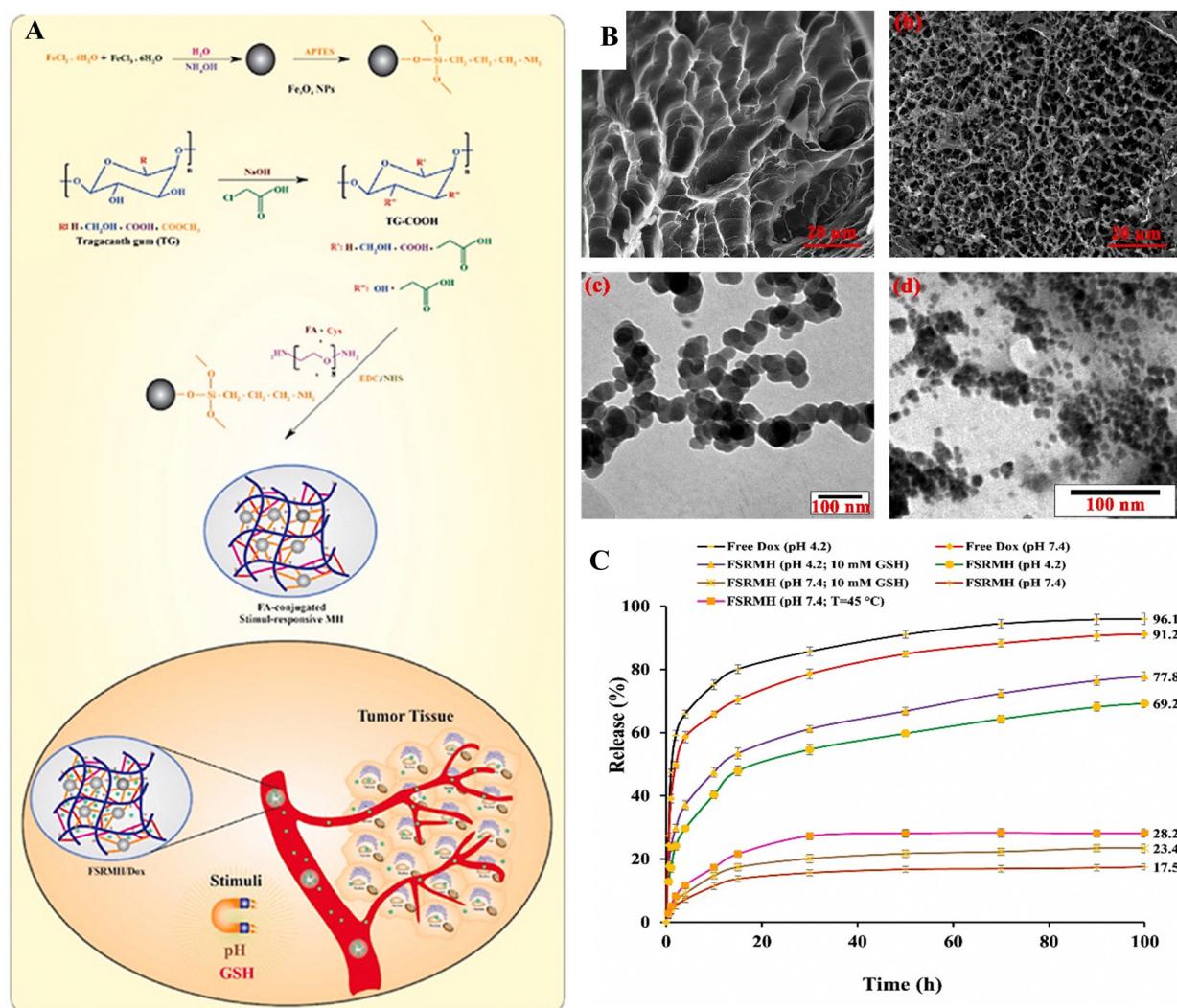
Fig. 18 (A) The synthetic pathway for producing FSRMH. (B) SEM images of native TG FSRMH and TEM images of FSRMH and Fe$_3$O$_4$–NH$_2$ nanoparticles. (C) The *in vitro* drug release profiles of the formulated FSRMH/Dox are evaluated under various conditions; temperature is set at 37 °C, except for FSRMH (pH 7.4; temperature = 45 °C). Reproduced from ref. 126 with permission from Elsevier, copyright 2023.

This journal is © The Royal Society of Chemistry 2023

J. Mater. Chem. B, 2023, **11**, 10538–10565 | **10557**

5. Application of stimulus–responsive polysaccharide nanohydrogels in drug delivery systems

Recently, an increasing body of evidence indicates that the utilization of nanotechnology in the field of medicine has the potential to greatly augment the efficacy of diagnostics and treatments for intricate diseases. This field of research is incessantly advancing, with new breakthroughs occurring almost daily. Among the various drug transport systems available, nanogels have garnered significant attention in view of their unique combination of nanoparticles and hydrogels, as they offer distinct advantages such as targeted and time-controlled delivery of bioactive substances.

The drug delivery system based on nanohydrogels has immense promise, primarily attributed to its key characteristics such as stability in encapsulation, intelligent discharge mechanisms, solubility in water, biodegradability, and biocompatibility.[127] These properties have paved the way for the advancement of functionalized nanoparticles, serving as carriers for drugs and therapeutics; they allow for targeted and controlled release at precise locations within the body. In recent years, nanotechnology has emerged as a promising avenue for addressing diverse medical conditions, including diabetes, cancer, etc. This section discusses the numerous biomedical applications of nanogels.

5.1. Cancer therapy by nanogels

Irrespective of any nation's level of development, cancer remains a major contributor to illness and mortality on a global scale. In the year 2020, around 19.3 million individuals will have been diagnosed with new cases of cancer, resulting in nearly 10 million deaths worldwide.[128] Emphasizing the significance of prevention, early detection, and efficient cancer treatments is of utmost importance. In the field of cancer therapy, targeted drug delivery to precise tumor locations is a crucial strategy, and researchers are exploring various promising approaches. The exploitation of nanogels as drug delivery systems (DDSs) is one such significant strategy. Nanogels, which possess the combined attributes of hydrogels and nanoparticles, have immense potential as targeted DDSs in cancer therapy (Table 2). These versatile systems exhibit a modifiable porous structure and a particle size ranging from 20 to 200 nm, making them well-suited for effective drug delivery.[4,129] Nanogels demonstrate excellent stability and possess a significant capacity for drug loading, besides being amenable to customization to actively target specific disease sites, leading to improved drug accumulation. Additionally, nanogels can be designed to respond to several internal or external stimuli, including pH, temperature, light, or redox conditions. This enables the controlled and precise release of the loaded drug.[128]

5.2. Diabetes therapy by nanogels

In recent years, there has been a significant rise in the worldwide prevalence of diabetes mellitus. The 9th edition of the Diabetes Atlas, published by the International Diabetes Federation (IDF), reported an assessed global population of 463 million with diabetes in 2019. Projections indicate that this number is expected to increase to 578 million by 2030 and reach an astonishing 700 million by 2045. Currently, diabetes mellitus is considered a severe non-communicable disease, ranking closely behind cardiovascular disease and malignant tumors in terms of both mortality and morbidity rates. Diabetes mellitus, one of the

Table 2 Various nanogels, their response to stimuli for cancer therapy, and delivery of drugs

NG systems	Active therapeutic agent	NG size (nm)	Stimuli-responsive	Ref.
Sugarcane bagasse cellulose	Doxorubicin (DOX)	90 to 180	Redox/pH/thermal-responsiveness	11
Chitosan hydrochloride-carboxymethyl starch	Curcumin (Cu)	378	pH responsiveness	130
Hyaluronic acid (HA)	Doxorubicin (DOX)	22 to 433	Redox responsiveness	131
Carboxymethyl cellulose	Curcumin (Cu)	120 to 333	Enzyme responsiveness	132
Hyaluronic acid-g-7-N,N-diethylamino-4-hydroxymethylcoumarin (HA-CM)	Doxorubicin (DOX)	147 to 165	Light responsiveness (irradiated by a UVITRON INTELLI-RAY-400 system operated at 315–400 nm)	101
Protein/sodium alginate	Curcumin (Cu)	—	pH responsiveness	13
Poly-N-isopropylacrylamide (PNIPAM)	Indocyanine green (ICG)/5-fluorouracil (5-Fu)	808	Thermo responsiveness	133
Chitin	5-Fluorouracil (5-Fu)	120 to 140	pH responsiveness	134
2-(2 methoxyethoxy)ethyl methacrylate (MEO2MA)	Curcumin (Cu)	30 and 5	Thermo responsiveness	135
P(DEAEMA-co-HEMA-g-PEGMA)	SiRNA	71 to 111	pH and redox responsiveness	136
Chitosane-poly(N-isopropylacrylamide-co-acrylamide)	Paclitaxel	—	Thermo responsiveness	137
O-Carboxymethyl-chitosan/thiolated chitosan	Doxorubicin (DOX)	123 to 150	pH and redox responsiveness	138
Dex-SS	Doxorubicin (DOX)	592 nm	pH and redox responsiveness	34
Poly(N-isopropylacrylamide-maltodextrin)	Folic acid (FA)/resveratrol (RSV)	101 to 159	Thermo-/pH responsiveness	91
Chitosan/agarose/graphene oxide	5-Fluorouracil (5-Fu)	197	pH responsiveness	139
Alginate co-gold nanoparticles	Cisplatin	20 to 80	Thermo responsiveness	140
FCNGL	5-Fluorouracil (5-Fu)	100 to 250	pH responsiveness	141
4-Mercaptophenyle boronic acid/oxidized alginate	Doxorubicin (DOX)	155	pH and redox responsiveness	142
PVP	5-Fluorouracil (5-Fu)	41	pH responsiveness	143
Bovine serum albumin-gum arabic aldehyde (BSA-GAA)	5-Fluorouracil (5-Fu)	231	Thermo-/pH responsiveness	144

Table 3 Various nanogels, their response to stimuli for diabetes therapy, and delivery of drugs

NG systems	Therapeutics (drugs)	NG size (nm)	Stimuli-responsive	Ref.
Kappa-carrageenan/chitosan	Insulin	18 to 22	pH responsiveness	43
Concanavalin A/starch	Insulin	100 to 300	Glucose responsiveness	145
Oxidized starch	Exenatide	100 to 200	Glucose responsiveness	146
Dextran-4-carboxyphenylboronic acid-NIPAM	Insulin	160 300	Glucose responsiveness	96
Dextran	Insulin	293 to 340	Glucose responsiveness	147
P(NIPAM-co-Dex-co-DDOPBA)	Insulin	160 to 300	Glucose responsiveness	96
Methoxyl poly(ethylene glycol) acrylate and N-acryloyl-3-aminophenylboronic acid	Insulin	80 107	Glucose responsiveness	148
Carboxymethyl-hexanoly-chitosan-lysozyme	Insulin	40	Enzyme responsiveness	149
Hydroxypropyl methylcellulose methacrylic acid	Insulin	210 170	Thermo responsiveness	150
Chitosan-based luminescent/magnetic (CLM)	Insulin	160	Magnetic responsiveness	151

most common chronic ailments, is an endocrine and metabolic disorder distinguished by heightened levels of blood glucose (hyperglycemia) and the emergence of various complications.

An optimal smart insulin delivery system aims to promptly and accurately respond to fluctuations in blood sugar levels by delivering the appropriate dose of insulin. To fulfill these requirements, these systems must incorporate continuous glucose monitoring sensors and an insulin infusion pump. Consequently, these advanced systems are commonly referred to as glucose-responsive insulin delivery systems (Table 3).

5.3. Magnetic NG for hyperthermia

Superparamagnetic iron oxide nanoparticles (SPIONs), commonly referred to as magnetic-responsive nanoparticles or NGs, encompass a core comprising magnetite (Fe_3O_4) or maghemite (c-Fe_2O_3). These nanoparticles find diverse utility in numerous fields, such as magnetic resonance imaging (MRI), blood purification, pharmaceutical delivery, magnetic hyperthermia, *in vivo* biomarker detection using biosensors, and cell patterning. Unlike regular magnets, SPIONs lose their magnetism when not exposed to a magnetic field. The magnetic nanoparticles within NGs react to changes in a magnetic field, producing heat that plays a crucial role in pharmaceutical delivery. The toxicity of these products depends on factors

such as their shape, size, structure, and surface properties. By utilizing a focused magnetic field, magnetically responsive nanocarriers can be injected into solid tumors to enhance drug accumulation at the tumor sites (Table 4).

5.4. Photodynamic and photothermal therapy by nanogels

Phototherapies are rapidly advancing methods for treating cancer that utilize different wavelengths of light to create chemical or thermal changes in targeted tissues.[161] Photothermal therapy (PTT) and photodynamic therapy (PDT) are the primary categories of phototherapy (Table 5). Both PTT and PDT employ light along with either external or internal absorbers to induce the generation of cytotoxic reactive oxygen species (ROS) or localized temperature increases, respectively. These therapies can complement traditional cancer treatments by acting through unique mechanisms. At the cellular level, both PTT and PDT have displayed the capacity to circumvent chemotherapy resistance and compensate for signaling pathways. PTT and PDT can have effects on various aspects of the tumor microenvironment, including tumor blood flow, vascular permeability, and extracellular matrix permeability. These effects can be leveraged to improve the delivery of cancer medications to tumors. Additionally, PDT and PTT offer superior control over treatment location and timing when compared

Table 4 Various nanogels, their response to stimuli of magnetic hyperthermia, and delivery of drugs

NG systems	Therapeutics (drugs)	NG size (nm)	Stimuli-responsive	Ref.
Starch	Oncocalyxone A	143	Magnetic responsiveness	67
HA-CysNG@AuNR	Doxorubicin (DOX)	80 to 250	Redox responsiveness	131
Chitosan-g-PNVCL	Doxorubicin (DOX)	180 to 250	Thermo-/pH responsiveness	152
Poly(N-vinylcaprolactam) (PNVCL)/Fe_3O_4	5-Fluorouracil (5-Fu)	210 423	Thermo-/redox responsiveness	107
(Au/Fe_3O_4@PEG-b-P(DMAEMA-co-HEMA)-g-PNIPAAm)	Methotrexate (MTX)	50 92	Thermo-/pH responsiveness	153
MNP@DAS	Doxorubicin (DOX)	6–10 42–52	pH responsiveness	154
Chitosan-g-N-isopropylacrylamide	Doxorubicin (DOX)	30 to 50	Thermo-/pH responsiveness	155
Poly(N-isopropylacrylamide-co-acrylic acid)	Doxorubicin (DOX)	60 380	Thermo-/pH responsiveness	156
PLP	Doxorubicin (DOX)	121 163	Thermo responsiveness	157
Silk fibroin	Curcumin (CUR)	130 to 210	Magnetic/pH responsiveness	158
O-carboxymethylchitosan (O-CMCS)	Maleimides	4.2	Magnetic responsiveness	159
Alginate	Doxorubicin (DOX)	120 to 320	Magnet-, pH-, and reduction responsiveness	160

This journal is © The Royal Society of Chemistry 2023

J. Mater. Chem. B, 2023, 11, 10538–10565 | 10559

Table 5 Various nanogels, and their response to stimuli of photodynamic, photothermal therapy, and delivery of drugs

NG systems	Therapeutics (drugs)	NG size (nm)	Stimuli-responsive	Ref.
CS/PNIPAM	Gold	90–150	Magnetic and light (green light irradiation at 530 nm) responsiveness	25
PNIPAM/chitosan	Curcumin (CUR)	167	Thermo-/pH responsiveness	162
CS-g-poly(N-vinylcaprolactam)	Doxorubicin (DOX)	180 to 250	pH/thermo responsiveness	152
Hyaluronic acid/polypyrrole	Doxorubicin (DOX)	77	Light responsiveness (808 nm laser irradiation)	163
CS-GCNCs	5-Fluorouracil (5-Fu)	960	Light responsiveness (microwave irradiation)	164
Au nanoclusters-Cu^{2+}@sodium alginate/hyaluronic acid	HAuCl$_4$·4H$_2$O	193 275	Light responsiveness (light yellow)	165
NanoGold-core dendrimeric	Methotrexate (MTTX)	108 118	Light responsiveness (NIR laser-mediated at λ = 808 nm)	166
Chitosan	Gold	140	Light (irradiated alternately with a 655 nm laser light (20 J cm^{-2}) for PDT)/thermo responsiveness	167
DNA/TB	Cisplatin	175 236	Light responsiveness (irradiated by an LED light source (660 nm, 25 mW cm^{-2}))	168
Graphene/hyaluronic acid	Doxorubicin (DOX)	120	Light responsiveness (red color light emitted by graphene at 670 nm)	169
HTCCm-CECm-(HP-β-CD-A)	Paclitaxel (PTX)	305 308 336	pH responsiveness	170
ICG/PNIPAM	5-Fluorouracil (5-Fu)	—	Thermo responsiveness	133
CS-CD hydrid	Doxorubicin (DOX)	65 nm	pH responsiveness	171
(P(NIPAM-co-AAM))	Doxorubicin (DOX)	—	Light (near-infrared (NIR) light at 700 to 900 nm)/thermo responsiveness	172

to systemic therapies, thereby reducing the occurrence of off-target side effects. The latest developments in endoscopic and fiberoptic light delivery methods have enabled the precise targeting of solid tumors, even in anatomically sensitive areas where surgical procedures may not be viable. Significantly, phototherapies utilize nonionizing radiation, thus reducing the risk of secondary cancers compared to radiation therapy.

5.5. Gene delivery by nanogels

Gene interference technology, centered on gene silencing, has been explored as a potential treatment for genetically inherited diseases (Table 6). Established methods have utilized nanoassemblies, such as stimulus-responsive NGs, to transport siRNA, creating stable polyplexes with improved knockdown capabilities.

6. Toxicity of the nanohydrogels

The potential harm caused by nanohydrogels deployed in the drug delivery process is a significant issue. The chemical composition of polymer nanogels based on acrylate and methacrylate contains elements that may be harmful, making their routine medical use cumbersome. Furthermore, the presence of unreacted initiators, surfactants, monomers, and oligomers during the production of nanogels introduces additional challenges.

To address these issues, purification techniques have been investigated, including thorough rinsing of the end product and adjustments to improve polymerization speed. Additionally, alternative methods like gamma radiation and physical self-assembly have been explored for the preparation of nanogels, thus eliminating the requirement for cross-linking agents and polymerization initiators, strategies that have the potential to decrease toxicity levels. Various methods have been widely employed to evaluate the toxicity of hydrogels or nanogels, namely agar diffusion tests, direct contact, extract dilution, and cell culture techniques. Other tactics employed entail the creation of non-harmful nanogel systems by exploiting biocompatible and abundant natural polymers like pullulan, dextran, alginate, and hyaluronic acid as safer materials. Research findings indicate that cells exposed to these nanogels exhibit elevated rates of survival, thus indicating minimal toxicity.

7. Advantages of nanohydrogels

Nanogels possess exceptional features that make them excellent options for co-delivering drugs.[177] Their remarkable biocompatibility, stability, significant drug loading capacity, and the ability to release drugs in a controlled manner with environmental triggers render them optimal candidates for drug co-administration,[178] primarily due to:

Table 6 Various nanogels, their response to stimuli gene delivery therapy, and delivery of drugs

NG systems	Therapeutics (drugs)	NG size (nm)	Stimuli-responsive	Ref.
Dendritic polyglycerol/polyethylenimine	siRNA	79 ± 3	pH responsiveness	173
GS-AS1411/siRNA	siRNA	162.3, 216.5, and 234.9	Redox responsiveness	174
P(DEAEMA-co-HEMA-g-PEGMA)	siRNA	71.0 ± 0.7 to 524.6 ± 10.7 75.1 ± 3.4 to 699.5 ± 20.0	pH and redox responsiveness	136
Cationic glycol	siRNA	750 ($\sim$400 to 500)	Thermo responsiveness	175
PEI/PNIPAM	microRNA	50–70 and 20–40	Redox/pH responsiveness	176

1. Exceptional biocompatibility renders nanogels a highly promising avenue for drug delivery systems.[179]

2. The significant biodegradability of nanogels is vital in preventing the buildup of nanogel material within bodily organs, consequently mitigating toxicity and adverse effects.[180]

3. In the bloodstream and internal aqueous environment, nanogels remain inert, causing no immunological reactions within the body.[181]

4. Nanogels can be delivered through diverse methods, such as oral, pulmonary, nasal, parenteral, intra-ocular, and topical routes of administration.[182]

5. Nanogels are appropriate for delivering both water-loving (hydrophilic) and water-repelling (hydrophobic) medications, as well as charged substances and various diagnostic agents. This characteristic is greatly affected by the kinds of functional groups found in the interconnected polymer chains, the degree of crosslinking, and the specific crosslinking agent integrated into the polymeric structure.[183]

6. Nanogels exhibit a strong attraction to aqueous solutions, enabling them to expand or contract by absorbing water when placed in certain environments. This quality stands as the most advantageous aspect of nanogels, positioning them as excellent options for absorbing and transporting proteins, peptides, large biomolecules, and voluminous medications.[184]

7. The drug encapsulation within nanogels surpasses that of other nanocarriers and drug delivery systems, demonstrating notably superiority. This heightened loading capacity can be attributed to the impact of functional groups within the polymer structure. These functionalities create hydrogen bonds or similar weak connections within the polymer network, thus enhancing the capacity to load drugs or proteins by engaging with molecules at the interface.[182]

8. Integrating drugs into nanogels is a straightforward and natural process, often not dependent on specific chemical reactions. This characteristic streamlines the preparation of nanogels, as the drug doesn't have to be present in the initial stages of manufacturing. Instead, it can be introduced into the nanogel network in subsequent stages, particularly when the nanogels expand with water or aqueous biological fluids.[185]

9. Nanogels are engineered to release drugs in a controlled and consistent manner at the intended site, ultimately amplifying the drug's therapeutic effectiveness while mitigating any undesirable reactions.[186]

8. Conclusion and future perspective

Lately, there has been considerable attention directed towards nanocarriers within the realm of drug transport research. These nanocarriers have gained attention due to their diverse structures, which can be customized to package and transport loaded cargo to specific locations. Nanogels are a type of submicron hydrophilic polymeric network that exhibits good biocompatibility, high water absorption, and stability, besides offering intriguing possibilities for drug loading with minimal toxicity. The synthesis of nanogels is achievable through diverse methods, and the selection of a particular method influences the ultimate characteristics of the ensuing nanogel.

Overall, nanogels exhibit significant potential as vehicles for transporting drugs, offering promising prospects for intelligent drug delivery. The formulation of nanogels as optimal drug carriers should encompass several key attributes, including a high capacity for drug loading, an extended duration of circulation within the body, the presence of specific ligands that can be recognized by target cells, and the ability to degrade in response to specific stimuli. Undoubtedly, drug carriers play a vital role in tumor treatments by minimizing drug toxicity, enhancing therapeutic effectiveness, and improving patient tolerance. While numerous research endeavors have evaluated the effectiveness and safety of nanogel formulations, there is a scarcity of data regarding their long-term buildup and breakdown patterns. Thus, safety remains a principal apprehension for the prospective clinical use of nanogels. It's important to emphasize that a nanogel suitable for clinical use ought to be created using biocompatible and biodegradable materials, ensuring a chemistry that is safe and devoid of toxicity. Innovative design strategies, coupled with thorough *in vivo* investigations of nanogels, are pivotal in advancing them towards the clinical implementation.

In conclusion, we believe that polysaccharides-based nanocarriers represent a category of transporters that are straightforward to manufacture, feature a broad range of functions, and are economically viable. These carriers have significant promise for advancing precision medicine by enhancing targeted drug delivery to augment the drug absorption and mitigate drug-related toxicity. Additionally, these deliberations may serve as a catalyst for future investigations into the potential secondary effects, including potential side effects of drug-loaded polysaccharide-based nanogels. This exploration is crucial for optimizing this drug delivery system for eventual clinical application, especially with a focus on achieving anti-inflammatory effects.

Author contributions

Conflicts of interest

The authors declare no conflict of interest.

References

1 Y. Liang, M. Li, Y. Yang, L. Qiao, H. Xu and B. Guo, *ACS Nano*, 2022, **16**, 3194–3207.

2 M. Ghovvati, M. Kharaziha, R. Ardehali and N. Annabi, *Adv. Healthcare Mater.*, 2022, **11**, 2200055.

This journal is © The Royal Society of Chemistry 2023

J. Mater. Chem. B, 2023, **11**, 10538–10565 | **10561**

3   P. Wang, X. Meng, R. Wang, W. Yang, L. Yang, J. Wang, D. Wang and C. Fan, *Adv. Healthcare Mater.*, 2022, **11**(13), 2102818.

4   F. Damiri, S. Rojekar, Y. Bachra, R. S. Varma, S. Andra, S. Balu, C. V. Pardeshi, P. J. Patel, H. M. Patel, A. C. Paiva-Santos, M. Berrada and M. C. García, *J. Drug Delivery Sci. Technol.*, 2023, 104447.

5   H. Urakami, J. Hentschel, K. Seetho, H. Zeng, K. Chawla and Z. Guan, *Biomacromolecules*, 2013, **14**, 3682–3688.

6   M. Z. Quazi and N. Park, *Int. J. Mol. Sci.*, 2022, **23**, 1943.

7   *Nano Hydrogels*, ed. J. Jose, S. Thomas and V. K. Thakur, Springer Singapore, Singapore, 2021.

8   R. Mohammadinejad, H. Maleki, E. Larrañeta, A. R. Fajardo, A. B. Nik, A. Shavandi, A. Sheikhi, M. Ghorbanpour, M. Farokhi, P. Govindh, E. Cabane, S. Azizi, A. R. Aref, M. Mozafari, M. Mehrali, S. Thomas, J. F. Mano, Y. K. Mishra and V. K. Thakur, *Appl. Mater. Today*, 2019, **16**, 213–246.

9   A. O. Ijaola, D. O. Akamo, F. Damiri, C. J. Akisin, E. A. Bamidele, E. G. Ajiboye, M. Berrada, V. O. Onyenokwe, S.-Y. Yang and E. Asmatulu, *J. Biomater. Sci., Polym. Ed.*, 2022, 1–55.

10 J. K. Oh, D. I. Lee and J. M. Park, *Prog. Polym. Sci.*, 2009, **34**, 1261–1282.

11 Y. Pan, J. Liu, K. Yang, P. Cai and H. Xiao, *Mater. Sci. Eng., C*, 2021, **118**, 111357.

12 K. Lekjinda and P. Sunintaboon, *Carbohydr. Polym.*, 2023, **304**, 120495.

13 S. Shahbazizadeh, S. Naji-Tabasi and M. Shahidi-Noghabi, *Chem. Biol. Technol. Agric.*, 2022, **9**, 41.

14 T. Fernandes Stefanello, A. Szarpak-Jankowska, F. Appaix, B. Louage, L. Hamard, B. G. De Geest, B. van der Sanden, C. V. Nakamura and R. Auzély-Velty, *Acta Biomater.*, 2014, **10**, 4750–4758.

15 A. Kongprayoon, G. Ross, N. Limpeanchob, S. Mahasaranon, W. Punyodom, P. D. Topham and S. Ross, *Polym. Chem.*, 2022, **13**, 3343–3357.

16 M. Zhu, D. Lu, A. H. Milani, N. Mahmoudi, S. M. King and B. R. Saunders, *J. Colloid Interface Sci.*, 2022, **608**, 378–385.

17 S. Inphonlek, P. Sunintaboon, M. Léonard and A. Durand, *Carbohydr. Polym.*, 2020, **242**, 116417.

18 C. Guido, M. Testini, S. D'Amone, B. Cortese, M. Grano, G. Gigli and I. E. Palamà, *Mater. Adv.*, 2021, **2**, 310–321.

19 S. L. Mekuria, Z. Ouyang, C. Song, J. Rodrigues, M. Shen and X. Shi, *Bioconjugate Chem.*, 2022, **33**, 87–96.

20 N. K. Preman, S. Jain and R. P. Johnson, *ACS Omega*, 2021, **6**, 5075–5090.

21 A. A. Ali, A. Al-Othman and M. H. Al-Sayah, *J. Controlled Release*, 2022, **351**, 476–503.

22 S. Pardeshi, F. Damiri, M. Zehravi, R. Joshi, H. Kapare, M. K. Prajapati, N. Munot, M. Berrada, P. S. Giram, S. Rojekar, F. Ali, M. H. Rahman and H. R. Barai, *Polymers*, 2022, **14**, 3126.

23 N. K. Preman, R. R. Barki, A. Vijayan, S. G. Sanjeeva and R. P. Johnson, *Eur. J. Pharm. Biopharm.*, 2020, **157**, 121–153.

24 F. Mahmoodzadeh, M. Ghorbani and B. Jannat, *J. Drug Delivery Sci. Technol.*, 2019, **54**, 101315.

25 A. Pourjavadi, M. Doroudian, M. Bagherifard and M. Bahmanpour, *New J. Chem.*, 2020, **44**, 17302–17312.

26 T. Gabriel, A. Belete, G. Hause, R. H. H. Neubert and T. Gebre-Mariam, *J. Drug Delivery Sci. Technol.*, 2022, **75**, 103665.

27 M. Pooresmaeil and H. Namazi, *Int. J. Biol. Macromol.*, 2022, **200**, 247–262.

28 J. An, M. Liu, Z. Din, F. Xie and J. Cai, *Int. J. Biol. Macromol.*, 2023, **247**, 125697.

29 I. M. Alwaan, M. M. R. M. Jafar and Z. S. M. Allebban, *Biomed. Phys. Eng. Express*, 2019, **5**, 025021.

30 B. Massoumi, Z. Mozaffari and M. Jaymand, *Int. J. Biol. Macromol.*, 2018, **117**, 418–426.

31 M. Hesan, A. Gholipour-Kanani, M. Lotfi and M. Shafiee, *Biochem. Eng. J.*, 2023, **190**, 108742.

32 D. Qin, F. Wang, W. Sheng, S. Chang, H. Duan and L. Wang, *J. Iran. Chem. Soc.*, 2023, **20**, 921–930.

33 Y. Xue, X. Xia, B. Yu, X. Luo, N. Cai, S. Long and F. Yu, *RSC Adv.*, 2015, **5**, 73416–73423.

34 K. Yu, X. Yang, L. He, R. Zheng, J. Min, H. Su, S. Shan and Q. Jia, *Polymer*, 2020, **200**, 122585.

35 M. He, F. Teng, H. Chen, C. Wu, Y. Huang and Y. Li, *LWT*, 2022, **160**, 113259.

36 H. Su, X. Han, L. He, L. Deng, K. Yu, H. Jiang, C. Wu, Q. Jia and S. Shan, *Int. J. Biol. Macromol.*, 2019, **128**, 768–774.

37 L. Lin, W. Xu, H. Liang, L. He, S. Liu, Y. Li, B. Li and Y. Chen, *Colloids Surf., B*, 2015, **126**, 459–466.

38 G. Geyik, E. Güncüm and N. Işıklan, *Int. J. Biol. Macromol.*, 2023, **250**, 126242.

39 Q. Zeng, W. Zeng, Y. Jin and L. Sheng, *Food Chem.*, 2022, **367**, 130716.

40 A. G. Rusu, A. P. Chiriac, L. E. Nita, A. Ghilan, D. Rusu, N. Simionescu and L. M. Tartau, *Biochem. Eng. J.*, 2022, **179**, 108341.

41 Y.-T. Pan, Y.-F. Ding, Z.-H. Han, L. Yuwen, Z. Ye, G. S. P. Mok, S. Li and L.-H. Wang, *Carbohydr. Polym.*, 2021, **268**, 118257.

42 M. Zhang, S. Asghar, C. Tian, Z. Hu, Q. Ping, Z. Chen, F. Shao and Y. Xiao, *Carbohydr. Polym.*, 2021, **253**, 117194.

43 Z. Rahmani, M. Ghaemy and A. Olad, *Polym. Bull.*, 2021, **78**, 2709–2726.

44 O. Peleg-Evron, M. Davidovich-Pinhas and H. Bianco-Peled, *Int. J. Biol. Macromol.*, 2023, **227**, 654–663.

45 G. R. Bardajee, N. Khamooshi, S. Nasri and C. Vancaeyzeele, *Int. J. Biol. Macromol.*, 2020, **153**, 180–189.

46 W. Wu, W. Yao, X. Wang, C. Xie, J. Zhang and X. Jiang, *Biomaterials*, 2015, **39**, 260–268.

47 Y. K. Joung, J. Y. Jang, J. H. Choi, D. K. Han and K. D. Park, *Mol. Pharmaceutics*, 2013, **10**, 685–693.

48 N. T. Nguyen, Q. A. Bui, H. H. N. Nguyen, T. T. Nguyen, K. L. Ly, H. L. B. Tran, V. N. Doan, T. T. Y. Nhi, N. H. Nguyen, N. H. Nguyen, N. Q. Tran and D. T. Nguyen, *Gels*, 2022, **8**, 59.

49 G. D'Arrigo, C. Di Meo, E. Gaucci, S. Chichiarelli, T. Coviello, D. Capitani, F. Alhaique and P. Matricardi, *Soft Matter*, 2012, **8**, 11557.

50 H. S. Mahajan and P. P. Patil, *Indian J. Pharm. Educ. Res.*, 2017, **51**, S40–S45.

51 V. M. de, O. Cardoso, N. A. P. de Brito, N. N. Ferreira, F. I. Boni, L. M. B. Ferreira, S. G. Carvalho and M. P. D. Gremião, *Colloids Surf., A*, 2021, **628**, 127321.

52 W. Zhou, Z. Cai, R. Zhang, K. Hu, F. Wu, Y. Hu, C. Huang and Y. Chen, *Food Chem.*, 2023, **421**, 136143.

53 F. Pervaiz, W. Tanveer, H. Shoukat and S. Rehman, *Polym. Bull.*, 2023, **80**, 469–493.

54 J. Singh, S. Kumar and A. S. Dhaliwal, *J. Drug Delivery Sci. Technol.*, 2020, **55**, 101384.

55 A. Fatimi, O. V. Okoro, D. Podstawczyk, J. Siminska-Stanny and A. Shavandi, *Gels*, 2022, **8**, 179.

56 F. Damiri, Y. Bachra, C. Bounacir, A. Laaraibi and M. Berrada, *J. Chem.*, 2020, **2020**, 1–10.

57 A. Fatimi, P. Chabrot, S. Berrahmoune, J.-M. Coutu, G. Soulez and S. Lerouge, *Acta Biomater.*, 2012, **8**, 2712–2721.

58 T. Kean and M. Thanou, *Adv. Drug Delivery Rev.*, 2010, **62**, 3–11.

59 A. Fatimi, in *IOCN 2022*, MDPI, Basel Switzerland, 2022, p. 1.

60 Y. Yao, M. Xia, H. Wang, G. Li, H. Shen, G. Ji, Q. Meng and Y. Xie, *Eur. J. Pharm. Sci.*, 2016, **91**, 144–153.

61 A. Fatimi, J.-F. Tassin, R. Turczyn, M. A. V. Axelos and P. Weiss, *Acta Biomater.*, 2009, **5**, 3423–3432.

62 J. Kushwaha and R. Singh, *Inorg. Chem. Commun.*, 2023, **152**, 110721.

63 A. Fatimi, J. François Tassin, S. Quillard, M. A. V. Axelos and P. Weiss, *Biomaterials*, 2008, **29**, 533–543.

64 H. Ismail, M. Irani and Z. Ahmad, *Int. J. Polym. Mater.*, 2013, **62**, 411–420.

65 V. Vamadevan and E. Bertoft, *Starch - Stärke*, 2015, **67**, 55–68.

66 P. Guo, Y. Li, J. An, S. Shen and H. Dou, *Carbohydr. Polym.*, 2019, **226**, 115330.

67 A. C. C. Sousa, A. I. B. Romo, R. R. Almeida, A. C. C. Silva, L. M. U. Fechine, D. H. A. Brito, R. M. Freire, D. P. Pinheiro, L. M. R. Silva, O. D. L. Pessoa, J. C. Denardin, C. Pessoa and N. M. P. S. Ricardo, *Carbohydr. Polym.*, 2021, **264**, 118017.

68 R. Abka-khajouei, L. Tounsi, N. Shahabi, A. K. Patel, S. Abdelkafi and P. Michaud, *Mar. Drugs*, 2022, **20**, 364.

69 J. Sun and H. Tan, *Materials*, 2013, **6**, 1285–1309.

70 V. Urtuvia, N. Maturana, F. Acevedo, C. Peña and A. Díaz-Barrera, *World J. Microbiol. Biotechnol.*, 2017, **33**, 198.

71 M. Suhail, C.-W. Fang, I.-H. Chiu, A. Khan, Y.-C. Wu, I.-L. Lin, M.-J. Tsai and P.-C. Wu, *ACS Omega*, 2023, **8**, 23991–24002.

72 Y. Zhao and S. Jalili, *Int. J. Biol. Macromol.*, 2022, **207**, 666–682.

73 L. Liang, M. Xu, L. Pan, Z. Zhou and Y. Han, *Processes*, 2022, **10**, 891.

74 A. Noreen, Z.-H. Nazli, J. Akram, I. Rasul, A. Mansha, N. Yaqoob, R. Iqbal, S. Tabasum, M. Zuber and K. M. Zia, *Int. J. Biol. Macromol.*, 2017, **101**, 254–272.

75 D. Mohnen, *Curr. Opin. Plant Biol.*, 2008, **11**, 266–277.

76 B. L. Ridley, M. A. O'Neill and D. Mohnen, *Phytochemistry*, 2001, **57**, 929–967.

77 M. Zhou, T. Wang, Q. Hu and Y. Luo, *Food Hydrocolloids*, 2016, **57**, 20–29.

78 L. A. Pérez, R. Hernández, J. M. Alonso, R. Pérez-González and V. Sáez-Martínez, *Biomedicines*, 2021, **9**, 1113.

79 S. Luan, Y. Zhu, X. Wu, Y. Wang, F. Liang and S. Song, *ACS Biomater. Sci. Eng.*, 2017, **3**, 2410–2419.

80 D. Kang, H.-B. Zhang, Y. Nitta, Y.-P. Fang and K. Nishinari, *Polysaccharides*, Springer International Publishing, Cham, 2015, pp. 1–48.

81 X. T. Le and S. L. Turgeon, *Soft Matter*, 2013, **9**, 3063.

82 K. M. Rao, A. Kumar, A. Haider and S. S. Han, *Mater. Lett.*, 2016, **184**, 189–192.

83 S. Faria, C. L. de Oliveira Petkowicz, S. A. L. de Morais, M. G. H. Terrones, M. M. de Resende, F. P. de França and V. L. Cardoso, *Carbohydr. Polym.*, 2011, **86**, 469–476.

84 P. Jansson, L. Kenne and B. Lindberg, *Carbohydr. Res.*, 1975, **45**, 275–282.

85 L. M. Ferreira, M. H. M. Sari, J. H. Azambuja, E. F. da Silveira, V. F. Cervi, M. C. L. Marchiori, S. S. Maria-Engler, M. R. Wink, J. G. Azevedo, C. W. Nogueira, E. Braganhol and L. Cruz, *Invest. New Drugs*, 2020, **38**, 662–674.

86 S. Bhaladhare and S. Bhattacharjee, *Int. J. Biol. Macromol.*, 2023, **226**, 535–553.

87 H. Zheng, S. Wang, L. Zhou, X. He, Z. Cheng, F. Cheng, Z. Liu, X. Wang, Y. Chen and Q. Zhang, *Chem. Eng. J.*, 2021, **404**, 126439.

88 E. Rahmani, M. Pourmadadi, S. A. Ghorbanian, F. Yazdian, H. Rashedi and M. Navaee, *Eng. Life Sci.*, 2022, **22**, 634–649.

89 L. Rong, Y. Liu, Y. Fan, J. Xiao, Y. Su, L. Lu, S. Peng, W. Yuan and M. Zhan, *Carbohydr. Polym.*, 2023, **310**, 120721.

90 J. A. Luckanagul, C. Pitakchatwong, P. Ratnatilaka Na Bhuket, C. Muangnoi, P. Rojsitthisak, S. Chirachanchai, Q. Wang and P. Rojsitthisak, *Carbohydr. Polym.*, 2018, **181**, 1119–1127.

91 O. R. M. Metawea, M. Teleb, N. S. Haiba, A. O. Elzoghby, A. F. Khafaga, A. E. Noreldin, S. N. Khattab and H. H. Khalil, *Eur. Polym. J.*, 2023, **182**, 111721.

92 C. Yang, X. Wang, X. Yao, Y. Zhang, W. Wu and X. Jiang, *J. Controlled Release*, 2015, **205**, 206–217.

93 D. Gao, S. Asghar, J. Ye, M. Zhang, R. Hu, Y. Wang, L. Huang, C. Yuan, Z. Chen and Y. Xiao, *Carbohydr. Polym.*, 2022, **294**, 119785.

94 F. Damiri, Y. Bachra and M. Berrada, *Chin. J. Inorg. Anal. Chem.*, 2022, **50**, 100092.

95 T. Ye, X. Bai, X. Jiang, Q. Wu, S. Chen, A. Qu, J. Huang, J. Shen and W. Wu, *Polym. Chem.*, 2016, **7**, 2847–2857.

96 T. Elshaarani, H. Yu, L. Wang, L. Lin, N. Wang, K. Ur Rahman Naveed, L. Zhang, Y. Han, S. Fahad and Z. Ni, *Eur. Polym. J.*, 2020, **125**, 109505.

97 Q. Zong, R. Zhou, Z. Zhao, Y. Wang, C. Liu and P. Zhang, *Eur. Polym. J.*, 2022, **173**, 111217.

98 F. Damiri, N. Kommineni, S. O. Ebhodaghe, R. Bulusu, V. G. S. Sainaga Jyothi, A. A. Sayed, A. A. Awaji, M. O. Germoush, H. S. Al-malky, M. Z. Nasrullah, M. H. Rahman, M. M. Abdel-Daim and M. Berrada, *Pharmaceuticals*, 2022, **15**, 190.

This journal is © The Royal Society of Chemistry 2023

J. Mater. Chem. B, 2023, **11**, 10538–10565 | **10563**

99 D. Kulkarni, F. Damiri, S. Rojekar, M. Zehravi, S. Ramproshad, D. Dhoke, S. Musale, A. A. Mulani, P. Modak, R. Paradhi, J. Vitore, M. H. Rahman, M. Berrada, P. S. Giram and S. Cavalu, *Pharmaceutics*, 2022, **14**, 1097.

100 N. Wen, S. Lü, C. Gao, X. Xu, X. Bai, C. Wu, P. Ning and M. Liu, *Chem. Eng. J.*, 2018, **335**, 52–62.

101 C. Hang, Y. Zou, Y. Zhong, Z. Zhong and F. Meng, *Colloids Surf., B*, 2017, **158**, 547–555.

102 R. Messing, N. Frickel, L. Belkoura, R. Strey, H. Rahn, S. Odenbach and A. M. Schmidt, *Macromolecules*, 2011, **44**, 2990–2999.

103 B. Hermenegildo, C. Ribeiro, L. Pérez-Álvarez, J. L. Vilas, D. A. Learmonth, R. A. Sousa, P. Martins and S. Lanceros-Méndez, *Colloids Surf., B*, 2019, **181**, 1041–1047.

104 D. Fouad, Y. Bachra, G. Ayoub, A. Ouaket, A. Bennamara, N. Knouzi and M. Berrada, in *Chitin and Chitosan - Physicochemical Properties and Industrial Applications*, IntechOpen, 2020, pp. 1–24.

105 M. Khalil, A. Fahmi, N. M. Nizardo, Z. Amir and B. Mohamed Jan, *Langmuir*, 2021, **37**, 8855–8865.

106 A. Narmani and S. M. Jafari, *Carbohydr. Polym.*, 2021, **272**, 118464.

107 F. Gao, X. Wu, D. Wu, J. Yu, J. Yao, Q. Qi, Z. Cao, Q. Cui and Y. Mi, *Colloids Surf., A*, 2020, **587**, 124363.

108 W. Sun, T. Jiang, Y. Lu, M. Reiff, R. Mo and Z. Gu, *J. Am. Chem. Soc.*, 2014, **136**, 14722–14725.

109 F. Ding, Q. Mou, Y. Ma, G. Pan, Y. Guo, G. Tong, C. H. J. Choi, X. Zhu and C. Zhang, *Angew. Chem., Int. Ed.*, 2018, **57**, 3064–3068.

110 J. Li, C. Zheng, S. Cansiz, C. Wu, J. Xu, C. Cui, Y. Liu, W. Hou, Y. Wang, L. Zhang, I. Teng, H.-H. Yang and W. Tan, *J. Am. Chem. Soc.*, 2015, **137**, 1412–1415.

111 K. Lee, T. Kim, Y. M. Kim, K. Yang, I. Choi and Y. H. Roh, *Macromol. Rapid Commun.*, 2021, **42**, 2000457.

112 C. Yao, Y. Yuan and D. Yang, *ACS Appl. Bio Mater.*, 2018, **1**, 2012–2020.

113 M. C. Cochran, J. Eisenbrey, R. O. Ouma, M. Soulen and M. A. Wheatley, *Int. J. Pharm.*, 2011, **414**, 161–170.

114 C. Hernandez, S. Gulati, G. Fioravanti, P. L. Stewart and A. A. Exner, *Sci. Rep.*, 2017, **7**, 13517.

115 P. Shende and S. Jain, *J. Drug Targeting*, 2019, **27**, 1035–1045.

116 N. Rapoport, K.-H. Nam, R. Gupta, Z. Gao, P. Mohan, A. Payne, N. Todd, X. Liu, T. Kim, J. Shea, C. Scaife, D. L. Parker, E.-K. Jeong and A. M. Kennedy, *J. Controlled Release*, 2011, **153**, 4–15.

117 P. Wei, M. Sun, B. Yang, J. Xiao and J. Du, *J. Controlled Release*, 2020, **322**, 81–94.

118 N. Huebsch, C. J. Kearney, X. Zhao, J. Kim, C. A. Cezar, Z. Suo and D. J. Mooney, *Proc. Natl. Acad. Sci. U. S. A.*, 2014, **111**, 9762–9767.

119 S. Yamaguchi, K. Higashi, T. Azuma and A. Okamoto, *Biotechnol. J.*, 2019, **14**, 1800530.

120 P. Wei, E. J. Cornel and J. Du, *Drug Delivery Transl. Res.*, 2021, **11**, 1323–1339.

121 F. Maghsoudinia, H. Akbari-Zadeh, F. Aminolroayaei, F. F. Birgani, A. Shanei and R. K. Samani, *Eur. J. Pharm. Sci.*, 2022, **174**, 106207.

122 F. Q. Schafer and G. R. Buettner, *Free Radical Biol. Med.*, 2001, **30**, 1191–1212.

123 H. Sun, F. Meng, R. Cheng, C. Deng and Z. Zhong, *Expert Opin. Drug Delivery*, 2013, **10**, 1109–1122.

124 H. Wen, C. Dong, H. Dong, A. Shen, W. Xia, X. Cai, Y. Song, X. Li, Y. Li and D. Shi, *Small*, 2012, **8**, 760–769.

125 A. Degirmenci, H. Ipek, R. Sanyal and A. Sanyal, *Eur. Polym. J.*, 2022, **181**, 111645.

126 M. Eskandani, H. Derakhshankhah, R. Jahanban-Esfahlan and M. Jaymand, *J. Drug Delivery Sci. Technol.*, 2023, **84**, 104449.

127 A. Jha, A. Rama, B. Ladani, N. Verma, S. Kannan and A. Naha, *J. Appl. Pharm. Sci.*, 2021, **11**, 001–016.

128 A. A. Attama, P. O. Nnamani, O. B. Onokala, A. A. Ugwu and A. L. Onugwu, *Front. Pharmacol.*, 2022, **13**, 1–23.

129 C. I. Idumah, R. S. Odera, E. O. Ezeani, J. H. Low, F. A. Tanjung, F. Damiri and W. S. Luing, *Polym.-Plast. Technol. Mater.*, 2023, 1–26.

130 X.-M. Li, Z.-Z. Wu, B. Zhang, Y. Pan, R. Meng and H.-Q. Chen, *Food Chem.*, 2019, **293**, 197–203.

131 B. Li, Q. Xu, X. Li, P. Zhang, X. Zhao and Y. Wang, *Carbohydr. Polym.*, 2019, **203**, 378–385.

132 N. Tiwari, L. Nawale, D. Sarkar and M. Badiger, *Gels*, 2017, **3**, 8.

133 S. Yao, X. Jin, C. Wang, A. Cao, J. Hu, B. Chen and B. Wang, *J. Biomater. Appl.*, 2021, **36**, 565–578.

134 M. Sabitha, N. Sanoj Rejinold, A. Nair, V.-K. Lakshmanan, S. V. Nair and R. Jayakumar, *Carbohydr. Polym.*, 2013, **91**, 48–57.

135 A. Soto-Quintero, N. Guarrotxena, O. García and I. Quijada-Garrido, *Sci. Rep.*, 2019, **9**, 18187.

136 M. K. Notabi, E. C. Arnspang, N. A. Peppas and M. Ø. Andersen, *J. Drug Delivery Sci. Technol.*, 2023, **86**, 104510.

137 Y. Wang, H. Xu, J. Wang, L. Ge and J. Zhu, *J. Pharm. Sci.*, 2014, **103**, 2012–2021.

138 Y. Zuo, M. Kong, Y. Mu, C. Feng and X. Chen, *Int. J. Biol. Macromol.*, 2017, **104**, 157–164.

139 M. Rajaei, H. Rashedi, F. Yazdian, M. Navaei-Nigjeh, A. Rahdar and A. M. Díez-Pascual, *J. Drug Delivery Sci. Technol.*, 2023, **82**, 104307.

140 M. Mirrahimi, Z. Abed, J. Beik, I. Shiri, A. Shiralizadeh Dezfuli, V. P. Mahabadi, S. Kamran Kamrava, H. Ghaznavi and A. Shakeri-Zadeh, *Pharmacol. Res.*, 2019, **143**, 178–185.

141 P. Sahu, S. K. Kashaw, S. Sau, V. Kushwah, S. Jain, R. K. Agrawal and A. K. Iyer, *Colloids Surf., B*, 2019, **174**, 232–245.

142 S. Pillarisetti, V. Vijayan, J. Rangasamy, R. Bardhan, S. Uthaman and I.-K. Park, *J. Ind. Eng. Chem.*, 2023, **123**, 361–370.

143 A. Ges Naranjo, H. Viltres Cobas, N. Kumar Gupta, K. Rodríguez López, A. Artimez Peña, D. Sacasas and R. Álvarez Brito, *J. Mol. Liq.*, 2022, **362**, 119716.

144 G. Bashiri, S. A. Shojaosadati and M. Abdollahi, *Int. J. Biol. Macromol.*, 2021, **170**, 222–231.

145 R. Chang, M. Li, S. Ge, J. Yang, Q. Sun and L. Xiong, *Ind. Crops Prod.*, 2018, **112**, 98–104.

146 J. Bai, H. Zhang, Z. Yang, P. Li, B. Liu, D. Li, S. Liang, Q. Wang, Z. Li, J. Zhang, S. Chen, G. Hou and Y. Li, *J. Controlled Release*, 2022, **352**, 673–684.

147 Z. Gu, A. A. Aimetti, Q. Wang, T. T. Dang, Y. Zhang, O. Veiseh, H. Cheng, R. S. Langer and D. G. Anderson, *ACS Nano*, 2013, **7**, 4194–4201.

148 L. Zhao, C. Xiao, J. Ding, P. He, Z. Tang, X. Pang, X. Zhuang and X. Chen, *Acta Biomater.*, 2013, **9**, 6535–6543.

149 H.-S. Chou, M. Larsson, M.-H. Hsiao, Y.-C. Chen, M. Röding, M. Nydén and D.-M. Liu, *J. Controlled Release*, 2016, **224**, 33–42.

150 D. Zhao, X. Shi, T. Liu, X. Lu, G. Qiu and K. J. Shea, *Carbohydr. Polym.*, 2016, **151**, 1006–1011.

151 J.-M. Shen, L. Xu, Y. Lu, H.-M. Cao, Z.-G. Xu, T. Chen and H.-X. Zhang, *Int. J. Pharm.*, 2012, **427**, 400–409.

152 S. Indulekha, P. Arunkumar, D. Bahadur and R. Srivastava, *Colloids Surf., B*, 2017, **155**, 304–313.

153 M. Ghorbani, H. Hamishehkar, N. Arsalani and A. A. Entezami, *Mater. Sci. Eng., C*, 2016, **68**, 436–444.

154 N. Zohreh, S. Alipour, S. H. Hosseini, M. S. Xaba, R. Meijboom, M. F. Ramandi, N. Gholipour and M. Akhlaghi, *ACS Appl. Nano Mater.*, 2019, **2**, 853–866.

155 W. Pon-On, T. Tithito, W. Maneeprakorn, T. Phenrat and I.-M. Tang, *Mater. Sci. Eng., C*, 2019, **97**, 23–30.

156 W. Xiong, W. Wang, Y. Wang, Y. Zhao, H. Chen, H. Xu and X. Yang, *Colloids Surf., B*, 2011, **84**, 447–453.

157 S. Seo, C.-S. Lee, Y.-S. Jung and K. Na, *Carbohydr. Polym.*, 2012, **87**, 1105–1111.

158 W. Song, M. Muthana, J. Mukherjee, R. J. Falconer, C. A. Biggs and X. Zhao, *ACS Biomater. Sci. Eng.*, 2017, **3**, 1027–1038.

159 C. A. Demarchi, A. Debrassi, F. de Campos Buzzi, R. Corrêa, V. C. Filho, C. A. Rodrigues, N. Nedelko, P. Demchenko, A. Ślawska-Waniewska, P. Dłużewski and J.-M. Greneche, *Soft Matter*, 2014, **10**, 3441.

160 J. Huang, Y. Xue, N. Cai, H. Zhang, K. Wen, X. Luo, S. Long and F. Yu, *Mater. Sci. Eng., C*, 2015, **46**, 41–51.

161 M. Overchuk, R. A. Weersink, B. C. Wilson and G. Zheng, *ACS Nano*, 2023, **17**, 7979–8003.

162 F. Howaili, E. Özliseli, B. Küçüktürkmen, S. M. Razavi, M. Sadeghizadeh and J. M. Rosenholm, *Front. Chem.*, 2021, **8**, 1–17.

163 T. Xiao, W. Hu, Y. Fan, M. Shen and X. Shi, *Theranostics*, 2021, **11**, 7057–7071.

164 Y. Guo, Y. Chen, P. Han, Y. Liu, W. Li, F. Zhu, K. Fu and M. Chu, *Acta Biomater.*, 2020, **103**, 237–246.

165 Z. Yang, Z. Zhao, H. Cheng, Y. Shen, A. Xie and M. Zhu, *J. Colloid Interface Sci.*, 2023, **641**, 215–228.

166 S. Mahajan, N. Raval, D. Kalyane, N. Anup, R. Maheshwari, V. Tambe, K. Kalia and R. K. Tekade, *J. Drug Delivery Sci. Technol.*, 2020, **58**, 101814.

167 J.-Y. Kim, W. Il Choi, M. Kim and G. Tae, *J. Controlled Release*, 2013, **171**, 113–121.

168 H. Guo, H. Wang, H. Deng, Y. Zhang, X. Yang and W. Zhang, *Front. Bioeng. Biotechnol.*, 2023, **11**, 01–08.

169 Z. Khatun, M. Nurunnabi, M. Nafiujjaman, G. R. Reeck, H. A. Khan, K. J. Cho and Y. Lee, *Nanoscale*, 2015, **7**, 10680–10689.

170 Q. Song, Y. Yin, L. Shang, T. Wu, D. Zhang, M. Kong, Y. Zhao, S. He, S. Tan, Y. Guo and Z. Zhang, *Nano Lett.*, 2017, **17**, 6366–6375.

171 H. Wang, S. Mukherjee, J. Yi, P. Banerjee, Q. Chen and S. Zhou, *ACS Appl. Mater. Interfaces*, 2017, **9**, 18639–18649.

172 L. Yu, A. Dong, R. Guo, M. Yang, L. Deng and J. Zhang, *ACS Biomater. Sci. Eng.*, 2018, **4**, 2424–2434.

173 M. Dimde, F. Neumann, F. Reisbeck, S. Ehrmann, J. L. Cuellar-Camacho, D. Steinhilber, N. Ma and R. Haag, *Biomater. Sci.*, 2017, **5**, 2328–2336.

174 X. Zhao, Y. Xi, Y. Zhang, Q. Wu, R. Meng, B. Zheng and L. Rei, *Nanoscale Res. Lett.*, 2019, **14**, 273.

175 M. Ahmed, P. Wattanaarsakit and R. Narain, *Polym. Chem.*, 2013, **4**, 3829.

176 L. Liu, H. Yi, H. He, H. Pan, L. Cai and Y. Ma, *Biomaterials*, 2017, **134**, 166–179.

177 F. Pinelli, M. Saadati, E. N. Zare, P. Makvandi, M. Masi, A. Sacchetti and F. Rossi, *Int. Mater. Rev.*, 2023, **68**, 1–25.

178 Y. Yin, B. Hu, X. Yuan, L. Cai, H. Gao and Q. Yang, *Pharmaceutics*, 2020, **12**, 290.

179 L. Zha, B. Banik and F. Alexis, *Soft Matter*, 2011, **7**, 5908.

180 W. Xiao, J. Xiong, S. Zhang, Y. Xiong, H. Zhang and H. Gao, *Int. J. Pharm.*, 2018, **538**, 105–111.

181 G. D. Lewis Phillips, G. Li, D. L. Dugger, L. M. Crocker, K. L. Parsons, E. Mai, W. A. Blättler, J. M. Lambert, R. V. J. Chari, R. J. Lutz, W. L. T. Wong, F. S. Jacobson, H. Koeppen, R. H. Schwall, S. R. Kenkare-Mitra, S. D. Spencer and M. X. Sliwkowski, *Cancer Res.*, 2008, **68**, 9280–9290.

182 E. Anooj, M. Charumathy, V. Sharma, B. V. Vibala, S. T. Gopukumar, S. I. B. Jainab and S. Vallinayagam, *J. Mol. Struct.*, 2021, **1239**, 130446.

183 R. Ni, R. Feng and Y. Chau, *Life*, 2019, **9**, 59.

184 J. Peng, Q. Yang, Y. Xiao, K. Shi, Q. Liu, Y. Hao, F. Yang, R. Han and Z. Qian, *Adv. Funct. Mater.*, 2019, **29**, 1900004.

185 Z. Wang, N. Zhang, C. Chen, R. He and X. Ju, *J. Agric. Food Chem.*, 2020, **68**, 3607–3614.

186 R.-Q. Li, W. Wu, H.-Q. Song, Y. Ren, M. Yang, J. Li and F.-J. Xu, *Acta Biomater.*, 2016, **41**, 282–292.

This journal is © The Royal Society of Chemistry 2023

J. Mater. Chem. B, 2023, **11**, 10538–10565 | **10565**